Bethe stopping theory for a harmonic oscillator and Bohr's oscillator model of atomic stopping

Peter Sigmund
Fysisk Institut, Odense Universitet, DK-5230 Odense M, Denmark

Uffe Haagerup
Matematisk Institut, Odense Universitet, DK-5230 Odense M, Denmark

(Received 19 February 1986)

Bethe's expressions for the stopping cross section and the straggling parameter of a penetrating point charge have been evaluated for a spherical harmonic oscillator as a target. The results, which are rigorous except for the neglect of relativistic corrections and higher-order Born terms, are given in tabulated form as well as in the form of asymptotic shell-correction expansions to arbitrary order. Existing general expressions for the stopping cross section and straggling are confirmed as far as they go. The range of validity of various model theories of atomic stopping is tested. At velocities down to about the stopping maximum, the agreement is very good for the kinetic theory, while a Fermi gas with a properly chosen electron density yields a significantly different stopping maximum. The binary encounter theory underestimates the stopping power at all speeds. The dielectric or local-density approach does not reproduce the correct scaling behavior. None of the model theories reproduces the threshold behavior. For light projectiles, i.e., positrons and electrons, a Franck-Hertz-type structure is observed in the velocity dependence of the stopping cross section which is particularly pronounced near threshold. An equipartition rule is derived for contributions to the stopping cross section from low excitations, i.e., distant collisions, and close encounters. A straight extension of Bohr's oscillator model of atomic stopping is proposed which is shown to reproduce leading shell corrections in both stopping power and straggling and which, when applied to hydrogen, accurately describes the stopping power at velocities around and above the stopping maximum.

I. INTRODUCTION

The stopping of a point charge penetrating through matter at nonrelativistic speed is conventionally described by Bethe's theory[1] which is based on two main assumptions: (i) The stopping is caused by Coulomb excitation and ionization of the electrons of the stopping medium, and (ii) the interaction is treated within the first Born approximation. On the basis of these two assumptions, one obtains the following expression for the mean energy loss per path length (stopping power),[1-5]

$$-\frac{dE}{dx}=\frac{4\pi e_1^2 e^2}{mv^2}NZ_2L\ , \tag{1}$$

where e_1 and v are the projectile charge and speed, $-e$ and m the electron charge and mass, N is the number of target atoms or molecules per volume, Z_2 the number of electrons per target atom or molecule, and

$$L=\frac{mv}{\pi}\sum_n (E_n-E_0)\int\frac{d^3q}{q^4}\delta(E_n-E_0-\mathbf{q}\cdot\mathbf{v}+q^2/2m_1)\times|F_{n0}(\mathbf{q})|^2\ , \tag{2}$$

where m_1 is the projectile mass and E_n the energy of the target state $|n\rangle$, i.e.,

$$H|n\rangle=E_n|n\rangle\ , \tag{3}$$

H being the Hamiltonian describing one target atom or molecule; $\mathbf{q}$ is the momentum transfer to a target electron and

$$F_{n0}(\mathbf{q})=Z_2^{-1/2}\left\langle n\left|\sum_{j=1}^{Z_2}e^{i\mathbf{q}\cdot\mathbf{r}_j/\hbar}\right|0\right\rangle\ . \tag{4}$$

If the initial state $|0\rangle$ of the target is isotropic, (2) can be written in the more familiar form

$$L=\frac{1}{2}\sum_n (E_n-E_0)\int\frac{dQ}{Q^2}\langle|F_{n0}(\mathbf{q})|^2\rangle \tag{5a}$$

with the integration limits

$$\left|E_n-E_0+\frac{m}{m_1}Q\right|^2\le 2mv^2Q\ , \tag{5b}$$

where $\langle\ \rangle$ indicates an angular average, and

$$Q=q^2/2m\ . \tag{6}$$

The most familiar form of Bethe's stopping formula,

$$L\simeq\ln\left[\frac{2mm_1v^2}{(m+m_1)I}\right]\ , \tag{7}$$

where I is the mean excitation energy, is based on Eq. (5) and the following further assumption: (iii) The projectile speed v is much greater than the orbital speeds of the target electrons.

Deviations of Eq. (5) from Eq. (7) are called shell corrections.[2,6–13] At nonrelativistic speeds they are always significant except for light target atoms. Therefore, they need to be known if reliable values of I are to be extracted from experimental stopping data[14] in the velocity range where Eq. (7) is approximately correct. At low projectile speed, Eq. (7) does not even qualitatively apply.

Shell corrections have been determined from Eq. (5a) for hydrogenic wave functions.[7–10] The results are most appropriate for K electrons, but the procedure has also been applied to L and M electrons.[15–17] Moreover, series expansions of shell corrections in inverse powers of the projectile speed have been given,[2,6–9,13] and most recently, an ambitious attempt has been made to evaluate Eq. (5a) numerically on the basis of realistic atomic (or ionic) wave functions.[18] Shell corrections have also been evaluated for a model of a free-electron gas[19,20] and applied[21,22] to atomic systems by means of the local-density approximation.[12] Recently, shell corrections have been evaluated[23,24] on the basis of a kinetic theory[25] with the underlying assumption that the difference between Eqs. (5) and (7) is essentially due to the kinematics of the target electrons in their initial state.

Despite a substantial effort, considerable uncertainty prevails about the magnitude and dependence on projectile speed of shell corrections for all systems. This is most pronounced for heavy targets where, quite apart from relativistic effects, shell corrections are so large that series expansions do not even qualitatively apply. The accuracy of shell corrections based on hydrogenic wave functions is difficult to ascertain, as are those based on the electron-gas picture or the kinetic theory, the latter two in view of the lack of a realistic model of electronic binding forces. Finally, the numerical calculations of Ref. 18, although potentially correct, are still subject to doubt with regard to artifacts caused by rounding errors and the like.[26]

In view of this state of affairs, there is a strong motivation for a model calculation allowing a full investigation of the analytical structure of the stopping power, viz., shell corrections. The electron-gas model[19,20] comes closest to this requirement, yet the dielectric function derived in Ref. 19, apart from describing only approximately the properties of an electron gas, exhibits considerable analytic complexity and, moreover, describes electronic binding forces only rather indirectly via the plasma frequency.

We find it striking that the standard system for quantal model calculations, the harmonic oscillator, apparently never has been utilized to evaluate Eq. (5). This is even more striking in view of the fact that Bohr's pioneering as well as much subsequent work on stopping power relied on the classical harmonic oscillator.[27] Moreover, both the classical[28,29] and quantal[30,31] oscillator have served as model systems for theoretical investigations of higher-order e_1 effects, i.e., corrections to Eq. (5) from higher-order terms in the perturbation expansion.

In the following, we evaluate the stopping power as well as the related fluctuation (straggling) for an isotropic harmonic oscillator as a target. It is known that the excitation spectrum has Poisson form in suitable variables,[32] and it turns out that the stopping power and straggling can be expressed in terms of series or integrals that are simple enough to allow investigation of their analytical structure as well as determination of accurate values. One comes closest to an analytical expression in the case of a heavy projectile, $m_1 \gg m$, and in all cases, the range of validity of expansions valid at low and high speeds, respectively, can be determined.

With reliable expressions at hand for the stopping cross section and straggling parameter of an oscillator, we further explore Bohr's oscillator model of atomic stopping,[27,33,34] i.e., the replacement of an atom by an ensemble of harmonic oscillators. It will be shown that this picture describes the stopping behavior of an atom or molecule even substantially below the range of validity of the Bethe limit, Eq. (7).

II. STOPPING NUMBER FOR AN ISOTROPIC HARMONIC OSCILLATOR

We wish to evaluate Eqs. (4) and (5) for the case where H specifies a spherical harmonic oscillator with a resonance frequency ω. We note that, because of spherical symmetry, the direction of $\mathbf{q}$ in (5a) is arbitrary; hence it can be chosen to coincide with the z axis in a rectangular coordinate system. Thus, with the states $|n\rangle \equiv |n_x\rangle\,|n_y\rangle\,|n_z\rangle$, where $n_x,n_y,n_z = 0,1,2,\ldots$, only the terms with $n_x=n_y=0$ contribute to (5a), all other terms yielding zero matrix elements. By means of the generating function of Hermite polynomials,[35] one easily derives

$$\langle \nu | e^{iqz/\hbar} | 0 \rangle = \frac{1}{\sqrt{\nu!}} \left[i\frac{\sqrt{Q}}{\hbar\omega} \right]^{\nu} e^{-Q/2\hbar\omega} \tag{8}$$

with $\nu = n_z = 0,1,2,\ldots$, and hence, (5a) reads

$$L = \frac{1}{2} \sum_{\nu=1}^{\infty} \frac{1}{(\nu-1)!} \int d\xi\, \xi^{\nu-2} e^{-\xi} \tag{9}$$

with $\xi = Q/\hbar\omega$ and $E_n - E_0 = \nu\hbar\omega$. The limits of integration follow from Eq. (5b) which reads

$$(\nu + m\xi/m_1)^2 \le \xi/\epsilon \tag{10}$$

with $\epsilon = \hbar\omega/2mv^2$.

By comparison with Eq. (5a), we notice that the generalized oscillator strength[1,3]

$$f_{n0}(Q) = [(E_n - E_0)/Q]\,|F_{n0}(\mathbf{q})|^2$$

has Poisson form[32]

$$f_{n0}(Q) = \frac{1}{(n-1)!} \left[\frac{Q}{\hbar\omega} \right]^{n-1} e^{-Q/\hbar\omega}, \quad n = 1,2,3,\ldots$$

with a maximum (Bethe ridge[3]) at $Q = (n-1)\hbar\omega$. Evidently, the momentum-transfer spectrum is very narrow for close collisions ($n \gg 1$) at high speed and broad for dipole resonance excitation ($n = 1$), in agreement with the general picture.[1–3]

Consider first the case of a projectile much heavier than an electron, where Eq. (10) reads

$$\xi \ge \nu^2 \epsilon\,, \tag{11}$$

and hence, Eq. (9) yields

TABLE I. Stopping parameters of a spherical harmonic oscillator for a heavy projectile ($m_1 \gg m$). The first column shows the energy variable $\epsilon^{-1}=2mv^2/\hbar\omega$. The second and third columns show the stopping number L, Eq. (1), and the shell correction $-\Delta L$, Eq. (43), respectively. The fourth column shows the quantity $\epsilon L = S\hbar\omega/8\pi e_1^2 e^2$, S being the stopping cross section, and the last column shows M, Eq. (32), representing the ratio between straggling and the Bohr value.

$\frac{2mv^2}{\hbar\omega}$	L	$-\Delta L$	ϵL	M
0.10	0.000 00	−2.302 59	0.000 02	0.000 04
0.12	0.000 01	−2.120 28	0.000 11	0.000 22
0.14	0.000 05	−1.966 16	0.000 35	0.000 70
0.16	0.000 14	−1.832 72	0.000 85	0.001 69
0.18	0.000 30	−1.715 10	0.001 67	0.003 34
0.20	0.000 57	−1.610 01	0.002 87	0.005 74
0.25	0.001 89	−1.388 18	0.007 56	0.015 12
0.30	0.004 29	−1.208 26	0.014 29	0.028 59
0.35	0.007 84	−1.057 66	0.022 39	0.044 81
0.40	0.012 48	−0.928 77	0.031 20	0.062 51
0.45	0.018 11	−0.816 62	0.040 25	0.080 81
0.50	0.024 62	−0.717 77	0.049 24	0.099 14
0.60	0.039 80	−0.550 63	0.066 34	0.134 81
0.70	0.057 31	−0.413 99	0.081 87	0.168 51
0.80	0.076 62	−0.299 76	0.095 77	0.200 16
0.90	0.097 33	−0.202 69	0.108 14	0.229 89
1.00	0.119 16	−0.119 16	0.119 16	0.257 89
1.20	0.165 32	0.017 00	0.137 76	0.309 32
1.40	0.213 76	0.122 71	0.152 69	0.355 58
1.60	0.263 62	0.206 38	0.164 76	0.397 57
1.80	0.314 28	0.273 50	0.174 60	0.435 95
2.00	0.365 32	0.327 82	0.182 66	0.471 24
2.50	0.492 72	0.423 57	0.197 09	0.548 45
3.00	0.617 65	0.480 96	0.205 88	0.613 28
3.50	0.738 63	0.514 13	0.211 04	0.668 63
4.00	0.854 96	0.531 33	0.213 74	0.716 45
4.50	0.966 34	0.537 74	0.214 74	0.758 13
5.00	1.072 72	0.536 72	0.214 54	0.794 71
6.00	1.270 86	0.520 90	0.211 81	0.855 64
7.00	1.450 75	0.495 16	0.207 25	0.903 87
8.00	1.614 12	0.465 32	0.201 77	0.942 50
9.00	1.762 77	0.434 45	0.195 86	0.973 70
10.00	1.898 36	0.404 22	0.189 84	0.999 03
12.00	2.136 25	0.348 65	0.178 02	1.036 60
14.00	2.337 87	0.301 19	0.166 99	1.061 79
16.00	2.510 93	0.261 66	0.156 93	1.078 66
18.00	2.661 34	0.229 03	0.147 85	1.089 86
20.00	2.793 58	0.202 15	0.139 68	1.097 12
25.00	3.065 39	0.153 48	0.122 62	1.104 94
30.00	3.279 02	0.122 18	0.109 30	1.105 22
35.00	3.454 30	0.101 04	0.098 69	1.102 39
40.00	3.602 81	0.086 07	0.090 07	1.098 40
45.00	3.731 67	0.074 99	0.082 93	1.094 08
50.00	3.845 55	0.066 47	0.076 91	1.089 83
60.00	4.040 11	0.054 24	0.067 34	1.082 03
70.00	4.202 64	0.045 86	0.060 04	1.075 34
80.00	4.342 29	0.039 74	0.054 28	1.069 65
90.00	4.464 74	0.035 07	0.049 61	1.064 79
100.00	4.573 78	0.031 39	0.045 74	1.060 60
120.00	4.761 55	0.025 95	0.039 68	1.053 76
140.00	4.919 53	0.022 11	0.035 14	1.048 42
160.00	5.055 90	0.019 27	0.031 60	1.044 12
180.00	5.175 88	0.017 07	0.028 75	1.040 58
200.00	5.282 99	0.015 33	0.026 41	1.037 62
250.00	5.509 25	0.012 21	0.022 04	1.031 94
300.00	5.693 64	0.010 14	0.018 98	1.027 87

TABLE I. (*Continued*).

$\frac{2mv^2}{\hbar\omega}$	L	$-\Delta L$	ϵL	M
350.00	5.849 26	0.008 68	0.016 71	1.024 79
400.00	5.983 88	0.007 58	0.014 96	1.022 37
450.00	6.102 52	0.006 73	0.013 56	1.020 42
500.00	6.208 56	0.006 05	0.012 42	1.018 80
600.00	6.391 89	0.005 04	0.010 65	1.016 28
700.00	6.546 77	0.004 31	0.009 35	1.014 40
800.00	6.680 84	0.003 77	0.008 35	1.012 94
900.00	6.799 05	0.003 35	0.007 55	1.011 77
1000.00	6.904 74	0.003 01	0.006 90	1.010 80

$$-\epsilon\frac{dL}{d\epsilon}=\frac{1}{2}\sum_{\nu=1}^{\infty}\frac{(\nu^2\epsilon)^{\nu-1}}{(\nu-1)!}e^{-\nu^2\epsilon}\,. \tag{12}$$

This function has been plotted in Fig. 1. The function $L(\epsilon)$, evaluated by numerical integration, has been tabulated in Table I.

One may note that at low projectile speed, i.e., $\epsilon\gg 1$, only the leading term $\nu=1$ contributes to (12) or (9); hence, $dL/d\epsilon\sim -e^{-\epsilon}/2\epsilon$ or

$$L\sim\tfrac{1}{2}\mathrm{E}_1(\epsilon)\quad\text{for }\epsilon\gg 1\,, \tag{13}$$

where E_1 is the exponential integral $\mathrm{E}_1(\xi)=\int_{\xi}^{\infty}dt\,e^{-t}/t$. In particular, we have the obvious result that at low speed, only the lowest excitation level contributes to the stopping cross section. That contribution is also included in Fig. 1 (dashed line).

At high speed, or $\epsilon\ll 1$, Eq. (12) receives a contribution which approximately equals 0.5 from $\nu=1$ and another contribution from a range of ν values of the order of ϵ^{-1}, with an essentially empty interval in between. By means of Stirling's formula and approximation of the sum by an integral, it is easily seen that the latter contribution also approximately equals 0.5. This is a manifestation of the well-known equipartition rule[27,20] between dipole resonance excitation ($\nu=1$) and close Coulomb encounters ($\nu\hbar\omega\simeq 2mv^2$). A more quantitative formulation of that theorem will be given in Sec. XIII.

Equations (9) and (10) have also been evaluated for

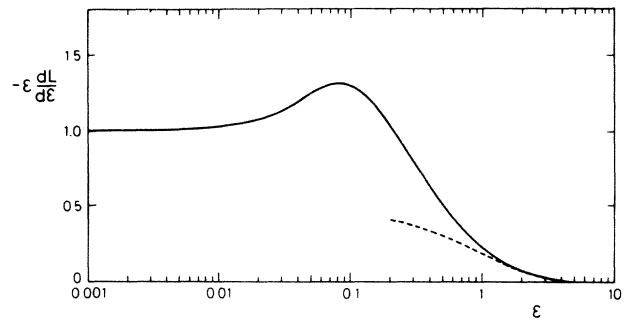

FIG. 1. Function $-\epsilon dL/d\epsilon$ for a heavy projectile, evaluated from Eq. (12). L is the stopping number, and $\epsilon=\hbar\omega/2mv^2$. Dashed line: excitation of lowest level only, Eq. (13).

$m_1=m$, i.e., when the projectile is a positron or an electron. The results, as shown in Table II, are more appropriate for positrons than for electrons, in view of the neglect of electron exchange in the case of the latter. Incorporation of exchange into the present model appears hard to do in a meaningful way in view of the lack of unbound states for a projectile electron.

III. ASYMPTOTIC EXPANSION OF THE STOPPING NUMBER FOR HEAVY PROJECTILES

In this section we derive an expansion of the stopping number of a harmonic oscillator for a heavy projectile, Eqs. (9) and (11),

$$L(\epsilon)=\frac{1}{2}\sum_{\nu=1}^{\infty}\frac{1}{(\nu-1)!}\int_{\nu^2\epsilon}^{\infty}dt\,t^{\nu-2}e^{-t}\,, \tag{9'}$$

in powers of ϵ or v^{-2}.

To find such an expansion is fairly straightforward for distant collisions, i.e., small Q, while there are pitfalls with regard to the high-Q portion. This confirms common experience.[2,13] In fact, we have explored several simple procedures which all failed to correctly reproduce the high-Q portion of the integral. The derivation given here makes use of integration in the complex plane of a meromorphic (multivalued) function. The reader who is only interested in the result may skip directly to Eq. (27).

We assume that $L(\epsilon)$ has an asymptotic expansion of the form

$$L(\epsilon)\sim a\ln\epsilon+b+\sum_{k=1}^{n}c_k\epsilon^k+R_n(\epsilon) \tag{14}$$

for small ϵ where $R_n(\epsilon)=O(\epsilon^{n+1})$. In order to find the coefficients a, b, and c_n, we consider the Mellin transform[36]

$$\bar{L}(s)=\int_0^{\infty}d\epsilon\,L(\epsilon)\epsilon^{s-1}\,. \tag{15}$$

$\bar{L}(s)$ is an analytic function defined in the full half-plane $\mathrm{Re}\,s>0$, because $L(\epsilon)$ decreases rapidly for $\epsilon\to\infty$, cf. Eq. (13).

Thus, for $\mathrm{Re}\,s>0$

$$\bar{L}(s)=-\frac{a}{s^2}+\frac{b}{s}+\sum_{k+1}^{n}\frac{c_k}{s+k}$$
$$+\int_0^1 d\epsilon\, R_n(\epsilon)\epsilon^{s-1}+\int_1^\infty d\epsilon\, L(\epsilon)\epsilon^{s-1}\,. \quad (16)$$

The last integral is an entire function of s, and the estimate $R_n(\epsilon)=O(\epsilon^{n+1})$ shows that the integral involving $R_n(\epsilon)$ is analytic for $\mathrm{Re}\, s<-(n+1)$. Hence $\bar{L}$ has an analytic continuation to $\mathrm{Re}\, s>-(n+1)$ with a second-order pole in $s=0$ and simple poles in $-s=1,2,\ldots,n$. Since n is arbitrary, (14) implies that $\bar{L}(s)$ can be extended to a meromorphic function in the full complex plane, with a second-order pole in 0 and simple poles in $-s=1,2,3,\ldots$. $\bar{L}(s)$ determines the coefficients a, b, and c_n, because the principal part of $\bar{L}(s)$ at 0 is $-a/s^2+b/s$, and for $n\geqq 1$, c_n is the residue of $\bar{L}$ at $s=-n$, i.e.,

$$c_n=\mathrm{Res}(\bar{L},-n)\,. \quad (17)$$

Let $L_\nu(\epsilon)$ be the part of $L_\nu(\epsilon)$ coming from the νth term in Eq. (9′). Then

$$\bar{L}_\nu(s)=\frac{1}{2(\nu-1)!}\int_0^\infty d\epsilon\,\epsilon^{s-1}\int_{\nu^2\epsilon}^\infty dt\, t^{\nu-2}e^{-t}$$
$$=\frac{1}{2(\nu-1)!}\int_0^\infty dt\, t^{\nu-2}e^{-t}\int_0^{t/\nu^2} d\epsilon\,\epsilon^{s-1}$$
$$=\frac{\nu^{-2s}}{2s(\nu-1)!}\Gamma(s+\nu-1)\,. \quad (16')$$

Using the identity

$$\nu^{-2s}=\frac{1}{\Gamma(2s)}\int_0^\infty dx\, e^{-\nu x}x^{2s-1} \quad (18)$$

we get

$$\bar{L}_\nu(\epsilon)=\frac{\Gamma(s)}{\Gamma(2s+1)}\binom{-s}{\nu-1}(-1)^{\nu-1}\int_0^\infty dx\, e^{-\nu x}x^{2s-1}\,.$$

Since

$$\sum_{\nu=1}^{\infty}(-1)^{\nu-1}\binom{-s}{\nu-1}e^{-\nu x}=(1-e^{-x})^{-s}e^{-x}\,,$$

we have shown that for $\mathrm{Re}\, s>0$

$$\bar{L}(s)=\sum_{\nu=1}^{\infty}\bar{L}_\nu(s)=\frac{\Gamma(s)}{\Gamma(2s+1)}\int_0^\infty dx\frac{e^{-x}}{x}\left[\frac{x^2}{1-e^{-x}}\right]^s$$
$$=\frac{\Gamma(s)}{\Gamma(2s+1)}\int_{-\infty}^0 dx\frac{e^{x}}{-x}\left[\frac{x^2}{1-e^{x}}\right]^s. \quad (19)$$

In the complex strip $|\mathrm{Im}\, z\,|<\pi$ with the negative real line excluded, we can choose the branch of the multivalued function

$$F_s(z)=\frac{e^z}{z}\left[\frac{z^2}{e^z-1}\right]^s \quad (20)$$

corresponding to the choice of argument:

$$-\pi<\arg\left[\frac{z^2}{e^z-1}\right]<\pi\,.$$

Let C be the complex contour specified in Fig. 2. For $x<0$, we have

$$\lim_{y\to 0\pm}F_s(x+iy)=\frac{e^x}{x}\left[\frac{x^2}{1-e^x}\right]^2 e^{\pm i\pi s}\,. \quad (21)$$

TABLE II. Stopping number L of a spherical harmonic oscillator for penetrating positrons (electrons).

$\frac{2mv^2}{\hbar\omega}$	L	$\frac{2mv^2}{\hbar\omega}$	L
1	0.000 00	51	3.120 56
2	0.000 00	52	3.134 41
3	0.000 00	53	3.173 40
4	0.000 00	54	3.191 75
5	0.356 12	55	3.206 24
6	0.492 76	56	3.218 85
7	0.593 21	57	3.254 84
8	0.674 79	58	3.271 69
9	0.918 90	59	3.284 98
10	1.034 89	60	3.296 57
11	1.124 47	61	3.329 99
12	1.199 15	62	3.345 57
13	1.379 40	63	3.357 85
14	1.470 22	64	3.368 56
15	1.541 65	65	3.399 77
16	1.602 01	66	3.414 25
17	1.741 21	67	3.425 67
18	1.812 37	68	3.435 63
19	1.868 78	69	3.464 90
20	1.916 83	70	3.478 44
21	2.028 18	71	3.489 10
22	2.084 95	72	3.498 41
23	2.130 08	73	3.525 98
24	2.168 74	74	3.538 69
25	2.260 46	75	3.548 70
26	2.306 75	76	3.557 44
27	2.343 59	77	3.583 48
28	2.375 27	78	3.595 46
29	2.452 68	79	3.604 89
30	2.491 28	80	3.613 13
31	2.521 98	81	3.637 82
32	2.548 45	82	3.649 15
33	2.615 16	83	3.658 06
34	2.648 00	84	3.665 86
35	2.674 09	85	3.689 32
36	2.696 65	86	3.700 07
37	2.755 12	87	3.708 52
38	2.783 58	88	3.715 92
39	2.806 15	89	3.738 28
40	2.825 71	90	3.748 50
41	2.877 70	91	3.756 54
42	2.902 75	92	3.763 57
43	2.922 59	93	3.784 93
44	2.939 80	94	3.794 67
45	2.986 59	95	3.802 34
46	3.008 93	96	3.809 05
47	3.026 60	97	3.829 48
48	3.041 96	98	3.838 80
49	3.084 49	99	3.846 12
50	3.104 64	100	3.852 53

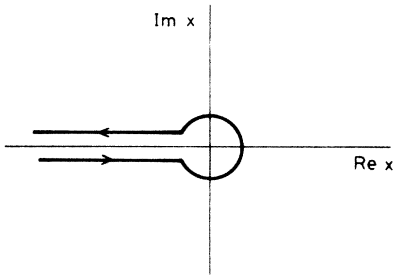

FIG. 2. Path of integration in Eq. (18) in the complex x plane.

Hence, for $\mathrm{Re}\, s > 0$,

$$\int_C F_s(z)dz = -2i \sin(\pi s) \int_{-\infty}^{0} dx \frac{e^x}{x} \left[\frac{x^2}{1-e^x} \right]^s$$

which shows that

$$\bar{L}(s) = \frac{\Gamma(s)}{\Gamma(2s+1)2i \sin(\pi s)} \int_C dz\, F_s(z), \quad \mathrm{Re}\, s > 0 . \tag{22}$$

However, the integral $\int_C F_s(z)dz$ is meaningful for all s and defines an entire function in complex s space. Thus, (21) shows that $\bar{L}(s)$ has an analytic continuation to the entire complex plane with poles in $0, -1, -2, -3, \ldots$. The pole at $s=0$ is at most a second-order pole and the poles at $-1, -2, -3, \ldots$ are all simple, because $\Gamma(s)/\Gamma(2s+1)$ has removable singularities at these points.

Since

$$\lim_{s \to -n} \frac{\Gamma(s)}{\Gamma(2s+1)} = \frac{(-1)^{n-1} \times 2[(2n-1)!]}{n!}$$

it follows from (17) that

$$c_n = -\frac{2(2n-1)!}{n!} \frac{1}{2\pi i} \int_C dz\, F_{-n}(z) . \tag{23}$$

When $s = -n$, the branch point 0 for $F_s(z)$ is just an nth-order pole, so the contour C can be deformed into a circle around the origin.

Therefore,

$$c_n = -\frac{(2n)!}{n(n!)} \mathrm{Res}(F_{-n}(z), 0)$$

$$= -\frac{(2n)!}{n(n!)} \mathrm{Res} \left[\frac{e^z(e^z-1)^n}{z^{2n+1}} \right] .$$

Using the Taylor expansion[37]

$$(e^z-1)^p = p! \sum_{q=0}^{\infty} \mathcal{S}_q^{(p)} \frac{z^q}{q!}, \quad p,q \geq 0$$

we get

$$\mathrm{Res} \left[\frac{(e^z-1)^p}{z^{q+1}}, 0 \right] = \frac{p!}{q!} \mathcal{S}_q^{(p)} ,$$

where $\mathcal{S}_q^{(p)}$ are the Stirling numbers of the second kind. This, combined with the recurrence formula[37]

$$\mathcal{S}_{q+1}^{(p+1)} = (p+1)\mathcal{S}_q^{(p+1)} + \mathcal{S}_q^{(p)} ,$$

yields

$$\mathrm{Res} \left[\frac{e^z(e^z-1)^p}{z^{q+1}}, 0 \right] = \mathrm{Res} \left[\frac{(e^z-1)^{p+1} + (e^z-1)^p}{z^{q+1}}, 0 \right]$$

$$= \frac{p!}{q!} \mathcal{S}_{q+1}^{(p+1)}$$

and therefore

$$c_n = -\frac{1}{n} \mathcal{S}_{2n+1}^{(n+1)}, \quad n = 1, 2, \ldots . \tag{24}$$

In order to determine the numbers a and b, we use that $-a/s^2 + b/s$ is the principal part of $\bar{L}(s)$ at $s=0$. Let $\phi'(0)$ be the first derivative of

$$\phi(s) = \frac{1}{2\pi i} \int_C dz\, F_s(z)$$

at $s=0$. Using $\Gamma(s) = \Gamma(s+1)/s$ and $\Gamma(s+1) = 1 - \gamma s + O(s^2)$, where γ is Euler's constant, we have

$$\bar{L}(s) = \frac{\Gamma(s)\phi(s)}{\Gamma(2s+1)[(1/\pi)\sin(\pi s)]}$$

$$= \frac{1}{s} \frac{1 - \gamma s + O(s^2)}{1 - 2\gamma s + O(s^2)} \frac{\phi(0) + \phi'(0)s + O(s^2)}{s + O(s^3)}$$

$$= \frac{1}{s^2} (\phi(0) + [\phi'(0) + \gamma]s + O(s^2)) \quad \text{for } s \to 0 .$$

Therefore, $a = -\phi(0)$ and $b = \phi'(0) + \gamma$.

Clearly, $\phi(0) = \mathrm{Res}(F_0(z), 0) = 1$, i.e.,

$$a = -1 . \tag{25}$$

Moreover, using

$$\frac{\partial}{\partial s} F_s(z) \bigg|_{s=0} = \frac{e^z}{z} \ln \left[\frac{z^2}{e^z - 1} \right]$$

we get

$$\phi'(0) = \frac{1}{2\pi i} \int_C dz \frac{e^z}{z} \ln \left[\frac{z^2}{e^z-1} \right] .$$

However,

$$\frac{1}{2\pi i} \int_C dz \frac{e^z}{z} \ln \left[\frac{z}{e^z-1} \right] = 0$$

because the integrated function has a removable singularity at $z=0$, so after subtraction of this integral, we find that

$$\phi'(0) = \frac{1}{2\pi i} \int_C dz \frac{e^z}{z} \ln z .$$

The Euler integral for the Γ function

$$\Gamma(s) = \int_0^{\infty} dx\, e^x x^{s-1}, \quad \mathrm{Re}\, s > 0$$

can, as in formulas (20) and (21), be transformed to an integral along the complex contour specified in Fig. 2:

$$\Gamma(s) = \frac{1}{2i \sin(\pi s)} \int_C dz\, e^z z^{s-1} .$$

Hence

$$\int_C dz\, e^z z^{s-1} = 2i \sin(\pi s)\Gamma(s) = \frac{2\pi i}{\Gamma(1-s)} .$$

By uniqueness of analytic continuation, the formula holds for all s. We have now

$$\phi'(0) = \frac{1}{2\pi i}\left[\frac{d}{ds}\int_C dz\, e^z z^{s-1}\right]_{s=0}$$

$$= \frac{d}{ds}\left[\frac{1}{\Gamma(1-s)}\right]\Bigg|_{s=0}$$

$$= \Gamma'(1) = -\gamma ,$$

which shows that

$$b = 0 . \tag{26}$$

Hence, we have found the asymptotic expansion

$$L(\epsilon) \sim \ln\left(\frac{1}{\epsilon}\right) - \sum_{n=1}^{\infty} \mathfrak{S}_{2n+1}^{(n+1)} \frac{\epsilon^n}{n}$$

$$= \ln\left(\frac{1}{\epsilon}\right) - 3\epsilon - \tfrac{25}{2}\epsilon^2 - \tfrac{350}{3}\epsilon^3 - \tfrac{6951}{4}\epsilon^4 - \cdots . \tag{27}$$

Strictly speaking, we have only derived the formula under the assumption that $L(\epsilon)$ has an asymptotic expansion of the form (14). The proof of the existence will not be given here. It involves the inversion formula for the Mellin transformation

$$L(\epsilon) = \frac{1}{2\pi i}\int_{\sigma - i\infty}^{\sigma + i\infty} ds\, \epsilon^{-s}\bar{L}(s), \quad \sigma > 0$$

together with estimates of the magnitude of $\bar{L}(\sigma + it)$ for $t \to \infty$ when $\sigma < 0$.

By differentiation of (27), we obtain

$$-\epsilon\frac{dL}{d\epsilon} = 1 + 3\epsilon + 25\epsilon^2 + 350\epsilon^3 + \cdots . \tag{27'}$$

This expansion can be compared with Fig. 1. The result is shown in Fig. 3. The solid line is the exact result from Fig. 1, plotted in a linear scale, and the dashed lines labeled 0,1,2,3, represent the series (27'), truncated after the term $\epsilon^0, \epsilon^1, \epsilon^2, \epsilon^3$, respectively. It is evident that with a required accuracy of 1% in $\epsilon dL/d\epsilon$, the asymptotic (Bethe) expression 0, cf. Eq. (7), is adequate for $\epsilon \lesssim 0.003$; addition of the leading shell correction is adequate for $\epsilon \lesssim 0.015$, two shell corrections for $\epsilon \lesssim 0.025$, and three for $\epsilon \lesssim 0.05$. Evidently, the shell-correction *expansion* is useful only in the limit of high speed where shell corrections are small. This result confirms common experience.

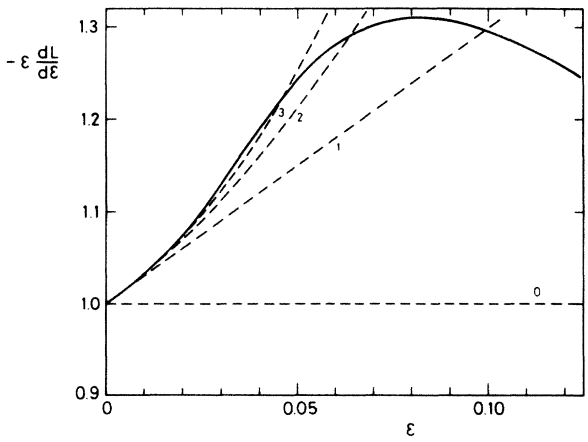

FIG. 3. Asymptotic behavior of $-\epsilon dL/d\epsilon$, cf. Fig. 1, at high speed, i.e., small ϵ. Solid line: exact result (Fig. 1). Dashed lines labeled 0,1,2,3 indicate the standard Bethe expression, Eq. (7), and extensions by j shell corrections ($j = 1,2,3$), respectively.

IV. STOPPING NUMBER FOR LIGHT PROJECTILES (POSITRONS AND ELECTRONS)

The asymptotic expansion of the stopping number given in Sec. III can be modified to cover the case where the mass ratio $\alpha = m/m_1$ is nonvanishing. Again, the reader interested only in the result may skip directly to Eq. (29).

From (9) and (10) we find the Mellin transform of the νth term

$$\bar{L}_\nu(s) = \frac{1}{2s(\nu-1)!}\int_0^\infty dt\, t^{\nu-2+s}(\nu+\alpha t)^{-2s}e^{-t} .$$

The identity (18) yields

$$\bar{L}_\nu(s) = \frac{\Gamma(s+\nu-1)}{\Gamma(2s+1)[(\nu-1)!]}\int_0^\infty dx \frac{x^{2s-1}}{(1+\alpha x)^{s+\nu-1}}e^{-\nu x} .$$

The summation over ν can now be carried out as in Sec. III and yields

$$\bar{L}(s) = \frac{\Gamma(s)}{\Gamma(2s+1)}\int_0^\infty \left[\frac{x^2}{1+\alpha x - e^{-x}}\right]^s \frac{e^{-x}}{x} dx$$

for $\mathrm{Re}\, s > 0$. From this we obtain

$$\bar{L}(s) = \frac{\Gamma(s)}{\Gamma(2s+1)2i\sin(\pi s)}\int_C dz\, F_s^\alpha(z) ,$$

where

$$F_s^\alpha(z) = \frac{e^z}{z}\left[\frac{z^2}{e^z - 1 + \alpha z}\right]^s .$$

Put

$$\phi_\alpha(s) = \int_C dz\, F_s^\alpha(z) .$$

Assume now that $L_\alpha(\epsilon)$ has an asymptotic expansion of the form (14). Then, as in Sec. III, one gets

$$a(\alpha) = -\phi_\alpha(0), \quad b(\alpha) = \phi_\alpha'(0) + \gamma$$

and

$$c_n(\alpha) = \frac{(2n)!}{n(n!)}\mathrm{Res}\left[\frac{e^z}{z}\left[\frac{e^z - 1 + \alpha z}{z^2}\right]^n, 0\right],$$

$$n = 1,2,\ldots .$$

Clearly,

$$\phi_\alpha(0) = \mathrm{Res}\left[\frac{e^z}{z}, 0\right] = 1$$

and

$$\phi'_\alpha(0)=\phi'(0)+\int_C dz\frac{e^z}{z}\ln\left[\frac{e^z-1}{e^z-1+\alpha z}\right]$$
$$=-\gamma+\ln\left[\frac{1}{1+\alpha}\right]$$

because $\phi'(0)=-\gamma$ (cf. Sec. III) and because $\ln[(e^z-1)/(e^z-1+\alpha z)]$ has a removable singularity at $z=0$, and the limit of the function for $z\to 0$ is $\ln[1/(1+\alpha)]$.

This shows that

$$a(\alpha)=-1,\quad b(\alpha)=-\ln(1+\alpha)\ .$$

Similar to Sec. III we find

$$c_n(\alpha)=-\frac{(2n)!}{n(n!)}\sum_{j=0}^{n}\begin{bmatrix}n\\j\end{bmatrix}\mathrm{Res}\left[\frac{e^z(e^z-1)^{n-j}}{z^{2n-j+1}}\right]\alpha^j$$
$$=-\frac{(2n)!}{n(n!)}\sum_{j=0}^{n}\frac{(n-j)!}{(2n-j)!}\mathfrak{S}^{(n-j+1)}_{2n-j+1}\alpha^j$$
$$=-\frac{1}{n}\sum_{j=0}^{n}\begin{bmatrix}2n\\j\end{bmatrix}\mathfrak{S}^{(n+1-j)}_{2n+1-j}\alpha^j\ . \tag{28}$$

The first few terms of the asymptotic expansion are therefore

$$L(\epsilon)\sim\ln\left[\frac{1}{\epsilon}\right]-\ln(1+\alpha)-(3+2\alpha)\epsilon$$
$$-\frac{25+28\alpha+6\alpha^2}{2}\epsilon^2-\cdots\ . \tag{29}$$

For $\alpha=0$ it reduces to Eq. (27), and for $\alpha=1$ we get

$$L(\epsilon)\sim\ln\left[\frac{1}{2\epsilon}\right]-5\epsilon-\tfrac{59}{2}\epsilon^2-\cdots\ . \tag{30}$$

In the case $\alpha\neq 0$ it is not so obvious that $L(\epsilon)$ has an asymptotic expansion of (18) because L is not a smooth function of ϵ. When $1/\epsilon$ increases through $4\alpha\nu$, i.e., $m_1v^2/2$ passes through $\nu\hbar\omega$, another excitation channel is opened. This causes square-root singularities of $L(\epsilon)$ near the points $1/\epsilon=4\alpha\nu$, $\nu=1,2,\ldots$ (cf. Fig. 4), and creates oscillations with amplitudes roughly of the size

$$K\epsilon\exp\left[\left(1-\frac{1}{\alpha}-\ln\alpha\right)\frac{1}{4\alpha\epsilon}\right]$$

(Appendix). For $\alpha\neq 1$, this amplitude decreases more rapidly than any power of ϵ for $\epsilon\to 0$, so the oscillation does not affect the asymptotic expansion of L. However, in the most interesting case $\alpha=1$, the amplitude of the oscillation is of order ϵ, and the asymptotic expansion breaks down. In the case $\alpha=1$, one should instead look for an asymptotic expansion of the form

$$L(\epsilon)\sim\ln\left[\frac{1}{2\epsilon}\right]-\sum_{n=1}^{\infty}g_n(1/\epsilon)\epsilon^n\ ,$$

where $g_1,g_2,\ldots$ are periodic functions of period 4. We refer to the Appendix for further discussion.

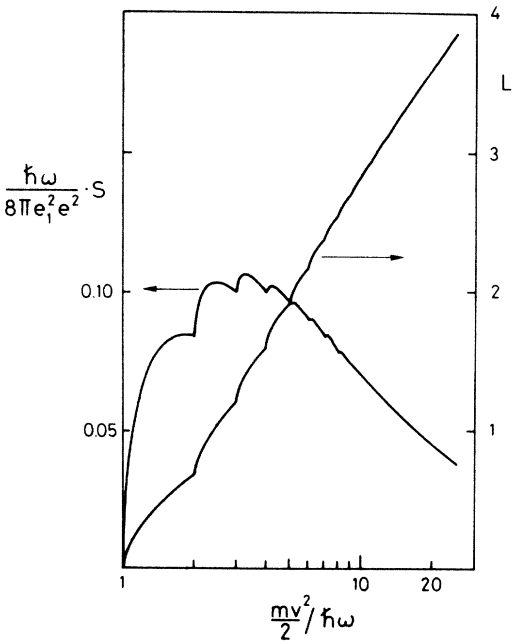

FIG. 4. Stopping of light projectiles, i.e., positrons and (neglecting exchange effects) electrons. Stopping number and stopping cross section vs relative kinetic energy, $mv^2/2\hbar\omega$.

For a target system that is well characterized by a harmonic oscillator, mainly the weak oscillatory structure for $\epsilon^{-1}\gtrsim 10$ will be of interest, while at low projectile energies, there may be little interest in characterizing the rather discrete energy-loss spectrum by its mean value.

Note, however, that the structure shown in Fig. 4 is very characteristic for the excitation spectrum of a harmonic oscillator and that, unlike many other results of the present work, generalization to atoms and molecules should be done with great caution.

V. STRAGGLING

Before discussing the above findings, we briefly report the corresponding results for the related problem of energy-loss fluctuation (straggling). According to elementary stopping theory,[2,5,6,33] the variance of energy loss per path length, $d\Omega^2/dx$, reads

$$\frac{d\Omega^2}{dx}=\frac{4\pi e_1^2e^2N}{2mv^2}\sum_n(E_n-E_0)^2\int\frac{dQ}{Q^2}\,|F_{n0}(\mathbf{q})|^2 \tag{31}$$

in analogy to Eqs. (1) and (5a) or, for a harmonic oscillator,

$$\frac{d\Omega^2}{dx}=4\pi e_1^2e^2NM(\epsilon) \tag{32}$$

with

$$M(\epsilon)=\epsilon\sum_{\nu=1}^{\infty}\frac{\nu}{(\nu-1)!}\int d\xi\,\xi^{\nu-2}e^{-\xi}\ . \tag{33}$$

Figure 5 shows the function M versus ϵ^{-1}. It has the qualitative behavior found in previous investigations.[6,25,38]

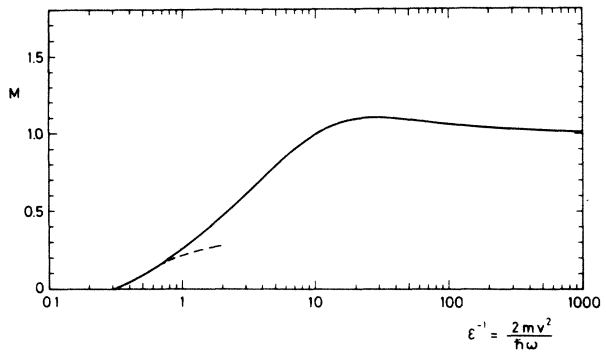

FIG. 5. Ratio M between straggling function of harmonic oscillator and Bohr's asymptotic (high-speed) result, for $m_1 \gg m$, from Eqs. (32) and (33). Dashed line: only first excitation level included, Eq. (34).

At low velocities, only the first excitation level contributes, and hence,

$$M(\epsilon) \sim \epsilon E_1(\epsilon) \quad \text{for } \epsilon \gg 1 \, . \tag{34}$$

This relation has also been included in Fig. 5.

Asymptotic expansion of $M(\epsilon)$ in powers of ϵ proceeds in complete analogy with the calculation presented in the foregoing sections and yields

$$M(\epsilon) = \left[\frac{1}{1+\alpha}\right]^2 + 2\epsilon\left[-\ln\epsilon - \ln(1+\alpha) - \frac{3+4\alpha}{2(1+\alpha)^2}\right] + \sum_{n=1}^{\infty} c_n(\alpha)\epsilon^n \, , \tag{35a}$$

where

$$c_n(\alpha) = -\frac{1}{n}\sum_{j=0}^{n}\binom{2n}{j}\mathfrak{S}_{2n+2}^{(n+1)}\alpha^j \, , \tag{35b}$$

i.e., for $\alpha = 0$ or heavy projectiles,

$$M \sim 1 + \frac{\hbar\omega}{mv^2}\left[\ln\left[\frac{2mv^2}{\hbar\omega}\right] - \frac{3}{2} - \frac{7}{2}\frac{\hbar\omega}{mv^2} - \cdots\right] , \tag{36}$$

and, for $\alpha = 1$ or $m_1 = m$,

$$M \sim \frac{1}{4} + \frac{\hbar\omega}{mv^2}\left[\ln\left[\frac{mv^2}{\hbar\omega}\right] - \frac{7}{8} - \frac{9}{2}\frac{\hbar\omega}{mv^2} - \cdots\right] . \tag{37}$$

As in case of the L function, the term $-\frac{9}{2}(\hbar\omega/mv^2)$ in (37) should be interpreted as the mean value of a term which has periodic oscillations in $1/\epsilon$.

VI. COMPARISON WITH KINETIC THEORY

The kinetic theory of stopping[25] is based on the assumption that shell corrections originate predominately in the kinematics of target electrons in their initial state, rather than the effect of their binding to the nuclei or each other on the collision dynamics. On the basis of binary collisions between the projectile and individual, free target electrons, the following expression has been derived[25] for the stopping cross section $S(v)$:

$$S(v) = \frac{\pi}{v^2}\int_0^\infty dv_2 v_2 f(v_2) \times \int_{|v-v_2|}^{v+v_2} dv'(v^2 - v_2^2 + v'^2) S_0(v') \tag{38}$$

for $m_1 \gg m$, where $f(v_2)$ is the (isotropic) velocity spectrum of target electrons, normalized according to $\int_0^\infty 4\pi v_2^2 dv_2 f(v_2) = 1$, and $S_0(v)$ the stopping cross section in the limit of $v \gg v_2$, i.e., high projectile speed compared with the speed of target electrons.

The kinetic theory provides an (approximate) estimate of $S(v)$ on the basis of the following choice of S_0:

$$S_0(v) = \begin{cases} \dfrac{4\pi e_1^2 e^2}{mv^2}\ln\left[\dfrac{2mv^2}{\hbar\omega}\right], & 2mv^2 > \hbar\omega \\ 0, & 2mv^2 < \hbar\omega \, . \end{cases} \tag{39}$$

Evidently, Eq. (39) represents the Bethe formula Eq. (7), valid at high speed, cf. assumption (iii) in the Introduction. Specifically, for a spherical harmonic oscillator, we insert

$$f(v_2) = \left[\frac{m}{\pi\hbar\omega}\right]^{3/2} e^{-mv_2^2/\hbar\omega} \, , \tag{40}$$

i.e., the velocity distribution for the ground state, which is easily found by Fourier transformation of the wave function.[35]

Also, a shell-correction expansion has been derived in Ref. 25,

$$L(v) = \ln\left[\frac{2mv^2}{\hbar\omega}\right] - \frac{\langle v_2^2\rangle}{v^2} - \frac{\langle v_2^4\rangle}{2v^4} - \cdots \, , \tag{41}$$

which, after evaluation of the moments $\langle v_2^{2n}\rangle$ by means of Eq. (40), reads

$$L(v) = \ln\epsilon^{-1} - 3\epsilon - \tfrac{15}{2}\epsilon^2 - \cdots \tag{42}$$

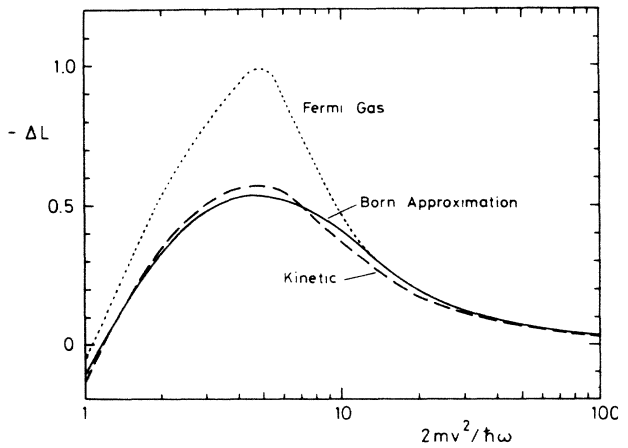

FIG. 6. Shell correction for spherical harmonic oscillator, heavy projectile, $m_1 \gg m$. $-\Delta L = \ln(2mv^2/\hbar\omega) - L$. Solid line: Born approximation, from Table I. Dashed line: kinetic theory, from Eqs. (38)–(40). Dotted line: Fermi gas, for density parameter $\chi^2 = e^2/\pi\hbar v_F = 0.12$.

(kinetic). This can be compared to the exact result (27).

Evidently, the leading terms in the shell-correction expansions agree, while the deviation in the second shell correction indicates that the kinetic theory underestimates the magnitude of the total shell correction slightly in the asymptotic limit.

Figure 6 shows the shell correction

$$\Delta L = L - \ln\left[\frac{2mv^2}{\hbar\omega}\right] \tag{43}$$

evaluated[39] by numerical integration of Eq. (38) after insertion of Eqs. (39) and (40), compared with the exact result from Table I. It is evident that despite the different analytic structure, there is very good agreement over the range of $2mv^2 \gtrsim \hbar\omega$. Note that the slight underestimate of the shell correction at high speed, mentioned above, turns into a slight overestimate for $2 \lesssim \epsilon^{-1} \lesssim 8$.

Figure 7 shows a comparison between the corresponding stopping cross sections. It is evident that the difference is less than 1.5% for $\epsilon^{-1} \gtrsim 10$ and $\lesssim 4\%$ near the maximum. At low speed, $\epsilon^{-1} < 1$, the difference becomes substantial. Indeed, the kinetic scheme yields $S \propto v$ at low speed (Fig. 8), while the Born approximation yields a threshold type of result, with an effective threshold at $\epsilon^{-1/2} \simeq 0.5$.

For straggling, the expression corresponding to Eq. (41) from the kinetic theory reads[25]

$$M = 1 + \frac{\langle v_2^2 \rangle}{v^2}\left[\frac{2}{3}\ln\left[\frac{2mv^2}{\hbar\omega}\right] - 1\right] + O(v^{-4}) \tag{36'}$$

or, after insertion of $\langle v_2^2 \rangle = 3\hbar\omega/2m$,

$$M = 1 + 2\epsilon\left[\ln\left[\frac{1}{\epsilon}\right] - \frac{3}{2}\right] + O(\epsilon^2)\,, \tag{36''}$$

in complete agreement with the exact result, Eq. (36).

This is an important finding: Up until now, the validity of the kinetic theory was tested mainly for the stopping power, while for straggling, considerable uncertainty prevailed because it did not strictly reproduce the straggling parameter of a free-electron gas.[25,40,41] The present result demonstrates that at least the leading correction to the Bohr straggling parameter is rigorously described by the kinetic scheme for the oscillator, i.e., a system characterized by the presence of a genuine binding force.

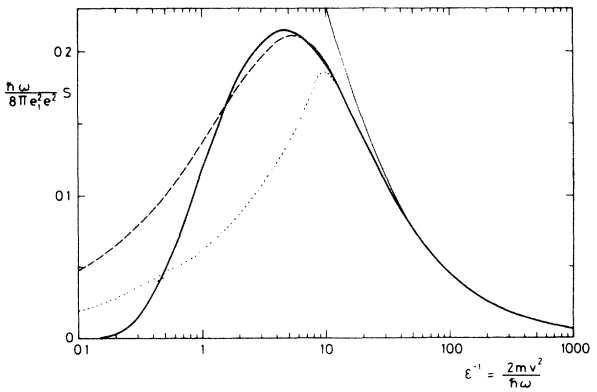

FIG. 7. Stopping cross section for spherical harmonic oscillator. Solid line: Born approximation, from Table I. Dashed line: kinetic theory (Ref. 39), from Eqs. (38)–(40). Dotted line: Fermi gas, for density parameter $\chi^2 = 0.12$.

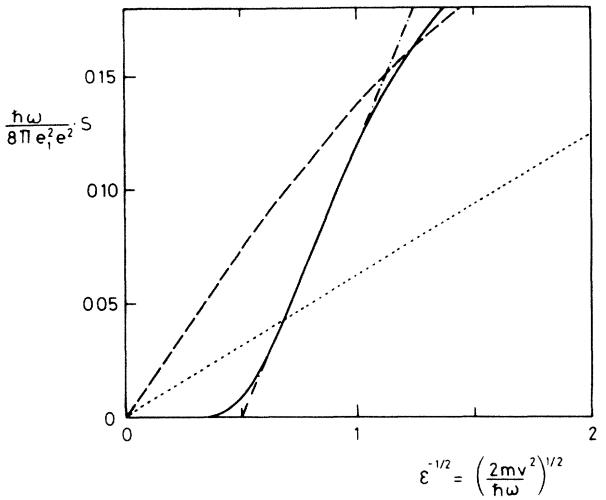

FIG. 8. Same as Fig. 7 with different abscissa scale. Dot-dashed line: straight-line extrapolation of solid curve.

The kinetic theory is distinctly different from the so-called binary-encounter theories;[42] in the latter, the classical Coulomb cross section is integrated from some threshold for excitation or ionization. This scheme is known to yield only half the Bethe stopping power in the high-speed limit,[43] but it has occasionally been claimed[44] that it describes the stopping power well in the region around and below the maximum. Figure 9 shows that the binary-encounter scheme, when applied to the harmonic oscilla-

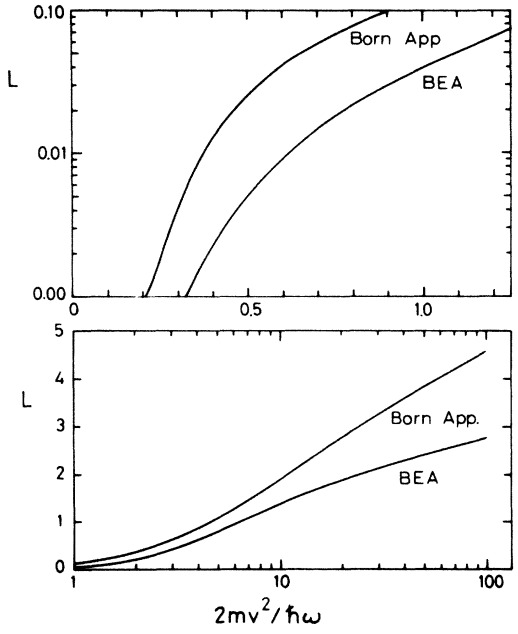

FIG. 9. Stopping number of a heavy projectile, $m_1 \gg m$, evaluated (Ref. 45) in binary-encounter model (Ref. 44) for harmonic oscillator with velocity spectrum Eq. (40) and minimum transferred energy $\hbar\omega$. The exact result from Table I has been included for comparison (Born approximation).

tor, underestimates the stopping power at all speeds. The discrepancy is largest below the stopping maximum and approaches a factor of 2 at high speed. Near the maximum ($\epsilon^{-1}\sim 5$), a $\sim 30\%$ difference is found.

A detailed analysis of the energy-loss spectrum[45] indicates that in the high-speed limit, the discrepancy between the binary-encounter model and the first Born approximation is due only to distant collisions, i.e, resonant excitations. This weakness is eliminated in the kinetic theory by basing the calculation on the asymptotic Bethe expression, cf. Eq. (39). The close-collision portion is known to be well described by the binary-encounter scheme.[41]

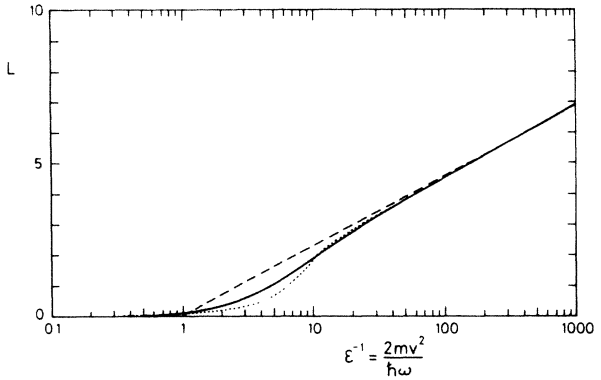

FIG. 10. Stopping number L for Fermi gas (dotted line); density parameter $\chi^2=0.12$. Interpolated from Ref. 20. Compared with harmonic-oscillator result from Table I (solid line) and Bethe logarithm Eq. (26) (dashed line).

VII. COMPARISON WITH FREE-ELECTRON GAS

The free-electron gas is a relevant issue in the present context to the extent that the stopping power of an electron gas is the basic tool in the dielectric theory of stopping.[12,21,22] In order to make a meaningful comparison with the present results we may follow two essentially different routes. In the first approach, we try to find a homogeneous electron gas with an appropriate density to match both the mean excitation energy and the velocity spectrum of target electrons as close as possible to that of a harmonic oscillator. In the second approach, we apply the local-density approximation to the electron-density distribution of a spherical harmonic oscillator.

We note that asymptotically, at high speed, the stopping number of an electron gas approaches[19] $L\sim\ln(2mv^2/\hbar\omega_p)$ for a heavy projectile, ω_p being the plasma frequency. Thus, the free-electron gas models a harmonic oscillator with eigenfrequency ω_p. The mean-square velocity of a degenerate Fermi gas is $\langle v_z^2\rangle=3v_F^2/5$, v_F being the Fermi speed, and for a harmonic oscillator in the ground state, we have $\langle v_z^2\rangle=3\hbar\omega/2m$. Hence, the appropriate condition to be imposed on the density of the electron gas reads

$$\frac{3}{5}v_F^2=\frac{3}{2}\frac{\hbar\omega_p}{m} \tag{44}$$

or

$$v_F=\frac{25}{3}\frac{e^2}{\pi\hbar}\ , \tag{45}$$

i.e., $\chi^2=e^2/\pi\hbar v_F=0.12$ in Lindhard's notation.[19,20] The curve of $L(2mv^2/\hbar\omega_p)$, interpolated from Ref. 20 for that particular Fermi speed, is shown in Fig. 10 together with the result for the harmonic oscillator in the Born approximation. Substantial deviations occur for $\epsilon^{-1}<10$. Note, however, that this comparison involves two different physical systems; in particular, despite Eq. (44), the velocity spectra are not identical.

A similar comparison can be performed in the case of straggling. In Ref. 40, The following asymptotic expression was derived for M on the basis of Ref. 19:

$$M=1+\left[\frac{v_F^2}{5v^2}+\frac{\hbar\omega_p}{2mv^2}\right]\ln\left[\frac{4mv^2}{\hbar\omega_p}\right]-\left[\frac{21}{40}\frac{v_F^2}{v^2}+\frac{\hbar\omega_p}{2mv^2}\right]+O(v^{-4})\ . \tag{46}$$

At the electron density quoted above, this yields

$$M=1+\frac{\hbar\omega_p}{mv^2}\left[\ln\left[\frac{2mv^2}{\hbar\omega_p}\right]-1.119\right]+O(v^{-4})\ ,$$

which differs from the oscillator result Eq. (36) only in the constant term in the square brackets.

The second approach, based on the local-density approximation,[12,21,22] expresses the stopping number L of a system by a weighted average

$$L=\int d^3r\,\rho(\mathbf{r})L(\rho(\mathbf{r}),v)\ , \tag{47}$$

the integral going over all space. Here, $L(\rho,v)$ is the stopping number of a homogeneous Fermi gas of density ρ, and $\rho(\mathbf{r})$ is the electron density corresponding to a harmonic oscillator in its ground state,[35]

$$\rho=\pi^{-3/2}\beta^3e^{-\beta^2r^2}\ , \tag{48}$$

with $\beta=(m\omega/\hbar)^{1/2}$.

According to Refs. 19 and 20,

$$L=-\frac{6}{\pi\chi^2}\int_0^{v/v_F}du\,u\int_0^\infty dz\,z\,\mathrm{Im}\left[\frac{1}{\epsilon(u,z)}-1\right]\ , \tag{49}$$

where $\epsilon(u,z)$, the dielectric function, reads

$$\epsilon(u,z)=1+\frac{\chi^2}{z^2}f(u,z)\ , \tag{50}$$

and $f(u,z)$ is a well-specified function of the integration variables u and z but independent of the density of the electron gas, all density dependence being contained in $\chi^2=e^2/\pi\hbar v_F$.

Inserting (49) and (50) into (47), and interchanging the order of integrations, we find

$$L=4.310\,\mathrm{Im}\int_0^\infty \frac{dz}{z}\int_0^\infty du\,uf\int_{x_0}^\infty dx\frac{x^2e^{-x^2}}{1+\frac{f}{z^2}e^{x^2/3}\left[0.03326\frac{e^2/a_0}{\hbar\omega}\right]^{1/2}}, \tag{51}$$

where $x=\beta\rho$ and

$$x_0=\max\left[0,\tfrac{3}{2}\ln\left[6.093u^2\frac{\hbar\omega}{2mv^2}\right]\right]. \tag{52}$$

This demonstrates that in the local-density approximation, the stopping number depends (through x_0) on the dimensionless quantity $2mv^2/\hbar\omega$ as it should, but also on the dimensionless parameter $(e^2/a_0)/\hbar\omega$ which is absent in the correct solution. The success of the dielectric theory in the quantitative prediction of stopping powers of atoms[21,22] suggests that this artifact is of minor significance as long as $\hbar\omega\leq e^2/a_0$.

While a detailed evaluation of (51) is outside the scope of the present paper, we may get instructive information from the high-speed limit, inserting the expansion[12,20]

$$L(\rho,v)\sim\ln\left[\frac{2mv^2}{\chi_{\mathrm{LS}}\hbar\omega_p}\right]-\frac{3}{5}\frac{v_F^2}{v^2}-\cdots \tag{53}$$

into Eq. (47). Here, χ_{LS} is a numerical constant introduced in Ref. 12 in order to qualitatively account for the lack of inclusion of binding forces in the dielectric theory.

Evaluation of (47) by means of the electron density (48) yields

$$L\sim\ln\left[\frac{2mv^2}{I'}\right]-1.699\frac{\hbar\omega}{2mv^2}+O((\hbar\omega/2mv^2)^2), \tag{54}$$

where

$$I'=\hbar\omega\frac{2}{\pi^{1/4}2.718^{3/4}}\left[\frac{e^2/a_0}{\hbar\omega}\right]^{1/4}\chi_{\mathrm{LS}}. \tag{55}$$

Equation (55) yields the correct value $I'=I=\hbar\omega$ if the constant χ_{LS} is chosen to be

$$\chi_{\mathrm{LS}}=1.409\left[\frac{\hbar\omega}{e^2/a_0}\right]^{1/4}. \tag{56}$$

We note that the constant 1.409 is very close to the value $2^{1/2}$ adopted in Ref. 12, yet the dimensionless factor $[\hbar\omega/(e^2/a_0)]^{1/4}$ confirms the lack of proper scaling inherent in the dielectric model, as mentioned above.

With regard to the leading term in the shell-correction expansion, Eq. (54) underestimates the correct expression $-3(\hbar\omega/2mv^2)$, Eq. (43), by almost a factor of 2. We note that in the local-density approximation, the first shell correction reads

$$-\frac{1}{v^2}\int d^3r\,\rho(\mathbf{r})\tfrac{3}{5}v_F^2(\rho(\mathbf{r}))$$

by means of Eq. (47). Here, the integral represents the local-density expression for the mean-square velocity of an atom. Thus, a sizable discrepancy in the first shell correction is equivalent with a discrepancy of the same magnitude in the mean-square velocity. This leads one to expect that the static Thomas-Fermi model would not be suited to describe a harmonic oscillator.

The discrepancy becomes more pronounced in the dielectric theory of straggling.[38,46,47] Starting from the asymptotic expression for the straggling parameter of an electron gas,[40] Eq. (46), we may integrate M over the density distribution of a harmonic oscillator in analogy with (47), but without including a parameter corresponding to χ_{LS} in Eq. (53). The result is

$$M(v)=1+\left[0.5663+\frac{0.8177}{\beta_0}\right]\epsilon\ln\left[\frac{\pi^{1/4}\beta_0}{\epsilon}\right]$$

$$-5.3974\epsilon-0.4089\frac{\epsilon}{\beta_0}+O(\epsilon^2)$$

with $\beta_0=[\hbar\omega/(e^2/a_0)]^{1/4}$ and $\epsilon=\hbar\omega/2mv^2$, which can be compared with (36). As in the case of the stopping power, this expression does not have the correct scaling behavior because of the occurrence of the factor β_0. In order to produce the correct logarithmic behavior one would have to choose $\beta_0=0.5703$. This choice would then generate a factor of 6.665 in front on the term proportional to ϵ, i.e., more than twice the exact value of 3.0.

The findings of this section will be discussed in Sec. XII.

VIII. EQUIPARTITION RULE

It was mentioned in Sec. II that in the limit of high projectile speed, the sum (12) receives equal contributions from $\nu=1$, i.e., dipole excitations, and a group of excitations around $\nu\sim\epsilon^{-1}$, i.e., close encounters. The present section serves to quantify this relationship. We consider the case of heavy projectiles only, i.e., $m_1\gg m$ or $\alpha=0$.

Consider again the Mellin transform $\bar{L}(s)$, Eq. (15). According to Eq. (27), its principal part at $s=0$ is $1/s^2$. On the other hand, according to Eq. (16'), the term $\nu=1$ in the sum (9') has the principal part $1/2s^2-\gamma/2s$ at $s=0$, γ being Euler's constant. Hence, the sum of the terms $\nu\geq 2$ must have the principal part $1/2s^2+\gamma/2s$ at $s=0$, although no single term in the infinite sum ($\nu\geq 2$) contributes to the principal part. Translated to $L(\epsilon)$ this reads

$$L_1(\epsilon)=\frac{1}{2}\ln\left[\frac{1}{\epsilon}\right]-\frac{\gamma}{2}+O(\epsilon),$$

$$\sum_{\nu=2}^{\infty}L_\nu(\epsilon)=\frac{1}{2}\ln\left[\frac{1}{\epsilon}\right]+\frac{\gamma}{2}+O(\epsilon),$$

i.e., there is equipartition for the logarithmic term but not for the constant. A similar equipartition rule holds for all terms proportional to ϵ^n ($n\geq 1$) in the asymptotic expansion of $L(\epsilon)$. To see this, observe that the residues of

$\bar{L}_\nu(s)$ at $-n$ vanish for $\nu > n+1$, while

$$\sum_{\nu=1}^{n+1} \mathrm{Res}[\bar{L}_\nu(s), -n] = -\frac{1}{2n}\sum_{\nu=1}^{n+1}\frac{\nu^{2n}}{(\nu-1)!}\mathrm{Res}[\Gamma(s), \nu-n-1] = \frac{1}{2n(n!)}\sum_{\nu=1}^{n+1}(-1)^{n-\nu}\begin{bmatrix} n \\ \nu-1 \end{bmatrix}\nu^{2n} . \quad (57)$$

Using $\binom{n}{\nu-1}+\binom{n}{\nu}=\binom{n+1}{\nu}$, and the formula for the Stirling numbers,[37]

$$\mathfrak{S}_n^{(m)} = \frac{1}{m!}\sum_{n=0}^{m}(-1)^{m-k}\begin{bmatrix} m \\ k \end{bmatrix}k^n , \quad (58)$$

we get

$$\sum_{\nu=1}^{n+1}\mathrm{Res}[\bar{L}_\nu(s), -n] = -\frac{1}{2n}[(n+1)\mathfrak{S}_{2n}^{(n+1)} + \mathfrak{S}_{2n}^{(n)}] = -\frac{1}{2n}\mathfrak{S}_{2n+1}^{(n+1)} . \quad (59)$$

Hence, the coefficient to ϵ^n in the asymptotic expansion of $\sum_{\nu=1}^{n+1} L_\nu(\epsilon)$ is exactly one-half the coefficient to ϵ^n in the expansion of $L(\epsilon)$ [cf. Eq. (24)]. Thus, we find the important result that both the Bethe logarithm and all orders of the shell-correction expansion receive equal contributions from low-lying excitations and from close encounters, while the constant term $-\gamma/2$ in $L_1(\epsilon)$ is canceled by a corresponding term $+\gamma/2$ arising from close encounters.

The present equipartition rule differs quantitatively from the one found for the Fermi gas[20] in the fact that the distant-collision contribution is made up by low excitation levels, such that the $n+1$ lowest excitation levels contribute to the nth term in the shell-correction expansion. Evidently, some overlap must eventually occur at lower projectile speeds between the two contributions. Conversely, for the Fermi gas, plasma-resonance excitation and single-particle excitation are strictly separated in the $\omega-q$ plane, i.e., the spectrum of energy versus momentum transfer.[20]

It is readily seen that as in the case of the electron gas,[20,25,40] the partition of the straggling parameter does not follow the simple rules found for the stopping power.

IX. EQUIVALENCE WITH ATOMIC CALCULATIONS

For an arbitrary atomic system, the following expression for the two first terms in the shell-correction expansion has been derived:[2,13]

$$\Delta L = -2\left[\frac{K_1}{2mv^2} + \frac{K_2}{(2mv^2)^2}\right] + O(v^{-6}) \quad (60)$$

with

$$K_1 = m\bar{v}_2^2 + \text{correlation terms} \quad (61a)$$

and

$$K_2 = m^2\bar{v}_2^4 + \frac{10\pi}{3}\frac{\hbar^2e^2}{m}\rho(0) + \text{correlation terms} , \quad (61b)$$

where mean values refer to the initial state, $\rho(0)$ is the electron density at the center of the atom, and correlation terms are absent when only one-electron systems are under consideration. We wish to demonstrate that (60) is consistent with Eq. (27).

We note first that according to (40),

$$\bar{v}_2^2 = \frac{3}{2}\frac{\hbar\omega}{m}, \quad \bar{v}_2^4 = \frac{15}{4}\left[\frac{\hbar\omega}{m}\right]^2 . \quad (62)$$

Moreover, the second term in (61b) reads, in more general form,

$$\frac{10\pi}{3}\frac{\hbar^2e^2}{m}\rho(0) = \frac{10\pi}{3}\frac{\hbar^2e^2}{m}\langle 0 \mid \delta(\mathbf{r}) \mid 0\rangle \Rightarrow \frac{10\pi}{3}\frac{\hbar^2e^2}{m}\left\langle 0\left|\frac{1}{4\pi e^2}\nabla^2 V\right|0\right\rangle \quad (63)$$

by means of Poisson's equation for a point charge e, where V is the potential energy.

Now, for a harmonic oscillator, $V=(m/2)\omega^2r^2$, and hence, (63) has to be replaced by

$$\frac{10\pi}{3}\frac{\hbar^2e^2}{m}\rho(0) \Rightarrow \frac{5}{6}\frac{\hbar^2}{m}\langle 0 \mid \nabla^2(m/2)\omega^2r^2 \mid 0\rangle = \tfrac{5}{2}(\hbar\omega)^2 . \quad (64)$$

After collecting Eqs. (61)–(64) and inserting them into (60) we find

$$\Delta L = -3\left[\frac{\hbar\omega}{2mv^2}\right]^2 - \frac{25}{2}\left[\frac{\hbar\omega}{2mv^2}\right]^2 - \cdots , \quad (65)$$

in complete agreement with Eq. (27).

For the case of straggling, the following result was given in Ref. 2,

$$M \sim 1 + \frac{2}{3}\frac{\langle v_2^2\rangle}{v^2}\ln\left[\frac{2mv^2}{I_1}\right] , \quad (66)$$

for a one-electron system in the nonrelativistic limit, with

$$\ln I_1 = \frac{\sum_n (E_n - E_0) f_n \ln(E_n - E_0)}{\sum_n (E_n - E_0) f_n} . \quad (67)$$

For a harmonic oscillator, we find $I_1 = \hbar\omega$, and hence,

$$M \sim 1 + \frac{\hbar\omega}{mv^2}\ln\left[\frac{2mv^2}{\hbar\omega}\right] , \quad (68)$$

i.e., the logarithmic correction agrees with the exact result, Eq. (36), but the nonlogarithmic correction term $-3\hbar\omega/2mv^2$ has been omitted in Ref. 2. This has been pointed out previously.[48]

X. OSCILLATOR MODEL OF ATOMIC STOPPING

According to Bethe,[1] the stopping number of an atom (or molecule) is given by

$$L_{\rm at}=\sum_n f_{n0}\ln\left[\frac{2mv^2}{E_n-E_0}\right] \tag{69}$$

in the high-speed limit, where E_n, $n=0,1,2,\ldots$, are the electronic energy levels and f_{n0} the dipole oscillator strengths,

$$f_{n0}=\frac{1}{Z_2}\frac{2m}{\hbar^2}(E_n-E_0)\left|\left\langle 0\left|\sum_j x_j\right|n\right\rangle\right|^2 . \tag{70}$$

It is tempting to generalize Eq. (69) to

$$L_{\rm at}=\sum_n f_{n0}L(2mv^2/(E_n-E_0)) , \tag{71}$$

where $L(2mv^2/\hbar\omega)$ is the stopping number of a harmonic oscillator (Table I). Equation (71) expresses the well-known fact that an atom to a certain extent may be regarded as an assembly of harmonic oscillators.[27,34]

To test the range of validity of Eq. (71), let us insert the shell-correction expansion (27) for L, i.e.,

$$L_{\rm at}=\sum_n f_{n0}\left[\ln\left[\frac{2mv^2}{E_n-E_0}\right]-3\frac{E_n-E_0}{2mv^2}-\frac{25}{2}\frac{(E_n-E_0)^2}{(2mv^2)^2}-\cdots\right] . \tag{72}$$

The leading term is evidently in agreement with (69), i.e., Eq. (71) is a correct expression for L in the limit of high projectile speed. For the first correction term, we utilize the sum rule

$$\sum_n f_{n0}(E_n-E_0)=\frac{2}{Z_2 m}\left\langle 0\left|\left[\sum_j p_{xj}\right]^2\right|0\right\rangle =\tfrac{2}{3}m\overline{v_2^2}+\text{correlation terms} , \tag{73}$$

which follows readily from (70). Hence, the first shell correction reads

$$K_1=m\overline{v_2^2}+\text{correlation terms} \tag{74}$$

in the notation of Eq. (60), in complete agreement with the general result Eq. (61a). Note that we do not have to restrict our attention to one-electron targets.

For the second shell correction, we need the sum rule

$$\sum_n f_{n0}(E_n-E_0)^2=\frac{1}{mZ_2}\left\langle 0\left|\left[\sum_j p_{xj},\left[V,\sum_j p_{xj}\right]\right]\right|0\right\rangle =\frac{4\pi}{3}\frac{\hbar^2e^2}{m}\rho(0)+\text{correlation terms} , \tag{75}$$

cf. Eq. (63). Hence, in the notation of Eq. (60), we find

$$K_2=\frac{25\pi}{3}\frac{\hbar^2e^2}{m}\rho(0)+\text{correlation terms} , \tag{76}$$

i.e., a result formally different from (61b).

However, for a hydrogen atom in the ground state, we have

$$\rho(0)=\frac{1}{\pi a_0^3},\quad \overline{v_2^4}=5\left[\frac{e^2}{ma_0}\right]^2 . \tag{77}$$

Inserting this into either (61b) or (76), we obtain

$$K_2=\frac{25}{3}\left[\frac{e^2}{a_0}\right]^2 \tag{78}$$

in both cases.

Thus, the ansatz (71), which is exact for the harmonic oscillator (where $f_{n0}=\delta_{n1}$), yields rigorously the first shell correction for any atomic or molecular target and even the second shell correction at least for a hydrogen atom in the ground state.

Now, we try the same ansatz for straggling. Similar to (71), set

$$M_{\rm at}=\sum_n f_{n0}M\left[\frac{2mv^2}{E_n-E_0}\right] . \tag{71'}$$

Inserting Eq. (36) for M yields

$$M_{\rm at}=\sum_n f_{n0}\left\{1+\frac{E_n-E_0}{mv^2}\left[\ln\left[\frac{2mv^2}{E_n-E_0}\right]-\frac{3}{2}-\frac{7}{2}\frac{E_n-E_0}{mv^2}-\cdots\right]\right\} \tag{79}$$

or, after insertion of Eqs. (73) and (75),

$$M_{\rm at}=1+\frac{\langle v_2^2\rangle}{v^2}\left[\frac{2}{3}\ln\left[\frac{2mv^2}{I_1}\right]-1\right]-\frac{14\pi}{3}\frac{\hbar^2e^2}{m}\frac{\rho(0)}{(mv^2)^2}+\text{correlation terms} \tag{80}$$

up to terms of order v^{-4}, where I_1 is defined by Eq. (67). Equation (80) agrees with the result of Ref. 2 as far as the latter goes, i.e., up to the logarithmic correction term. The constant $-\langle v_2^2\rangle/v^2$ is in agreement with the result given in Ref. 48. The v^{-4} term has not been evaluated previously to our knowledge. For a hydrogen atom, it reads

$$-\frac{14}{15}\frac{\langle v_2^4\rangle}{v^4} \tag{81}$$

by means of Eq. (77).

While (71) is by no means an exact relationship, it is tempting to investigate its range of validity in the case of a known system. The hydrogen atom is an obvious choice. With the known oscillator strengths,[1,3] we may evaluate the stopping number for atomic hydrogen in the form

$$L(x)=\sum_{n=2}^{\infty} f_n L(x/(1-1/n^2))+\int_0^\infty dt\, f(t)L(x/(1+t)) , \tag{82}$$

where $x=2mv^2/R$ and R is the Rydberg energy, n is the principal quantum number, and $t=E/R-1$ with E the excitation energy in the continuum. Moreover,

$$f_n=(2^8/3)n^5(n-1)^{2(n-2)}(n+1)^{-2(n+2)} \tag{83a}$$

and

$$f(t)=(2^7/3)(1+t)^{-4}(1-e^{-2\pi t^{-1/2}})^{-1}e^{-2g(t)t^{-1/2}} \tag{83b}$$

with

$$g(t)=\begin{cases}\arctan[2t^{1/2}/(1-t)], & t\le 1\\ \pi-\arctan[2t^{1/2}/(t-1)], & t\ge 1\ .\end{cases} \tag{83c}$$

An analogous expression has been evaluated for straggling. The results[49] are shown in Figs. 11 and 12. Figure 11 shows that the stopping number evaluated from Eq. (66) agrees very well with that evaluated directly from the Born approximation,[50] Eq. (5a), down to $2mv^2/I\sim 4$, $I=15.0$ eV being the mean excitation energy. An increasing discrepancy is observed at lower velocities. In that regime, higher-order Born terms are expected to be exceedingly important; hence, the uncertainty of *either* expression is not known. Also included in Fig. 11 is the stopping number of a harmonic oscillator with a resonance frequency $\omega=I/\hbar$. This curve has the correct asymptotic behavior in the Bethe asymptotic limit but does not reproduce the correct shell corrections. However, Fig. 11 indicates that the overall behavior of that curve is about as good in agreement with the Born-approximation result as is the one found from Eq. (66).

Figure 13 shows the excitation spectrum for atomic hydrogen along with the model spectrum employed in Eqs. (71) and (71′). To the left, discrete excitations A—D and excitations into the continuum E,F have been indicated. Note that now, as in Eq. (82), $n=1,2,\ldots$ is the principle quantum number. On the right, each column indicates one harmonic oscillator component, weighted in accordance with the appropriate dipole oscillator strength. Discrete transitions A'—D' are equivalent to A—D on the left-hand side. Also, transitions into the continuum E',F' occur which are equivalent to E and F. However, spurious effects occur due to higher transitions in the harmonic

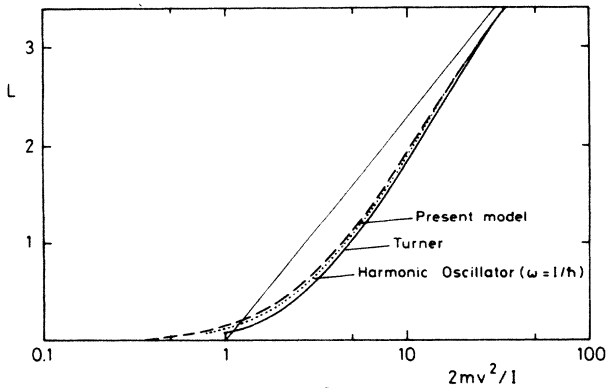

FIG. 11. Stopping number of atomic hydrogen. Solid line: Born approximation, Eq. (5a), Ref. 50. Dashed line: extended Bohr oscillator model, Eq. (66), Ref. 49. Dotted line: harmonic oscillator with frequency $\omega=I/\hbar$.

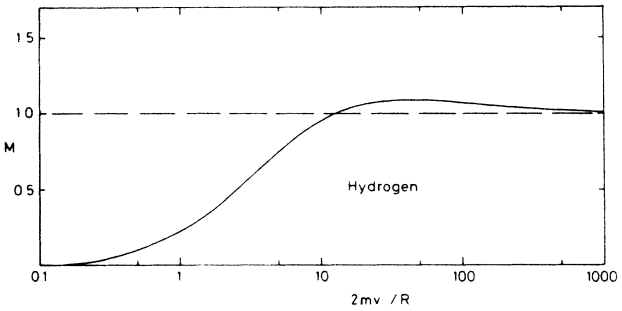

FIG. 12. Straggling for atomic hydrogen (Ref. 49). Extended Bohr oscillator model, Eq. (71′).

oscillators, such as G'. Such transitions have a vanishing dipole oscillator strength and therefore do not falsify the stopping cross section at high projectile speed where Eq. (69) is valid. At low speed, however, such transitions enter implicitly through the stopping number $L(2mv^2/(E_n-E_0))$ of the harmonic oscillator. It is evident from Fig. 13 that pronounced distortions of the excitation spectrum are to be expected mostly in the lower part of the continuum.

Note that at projectile speeds low enough for higher excitation levels to be insignificant (cf. dashed lines in Figs. 1 and 5), the oscillator model properly describes the exci-

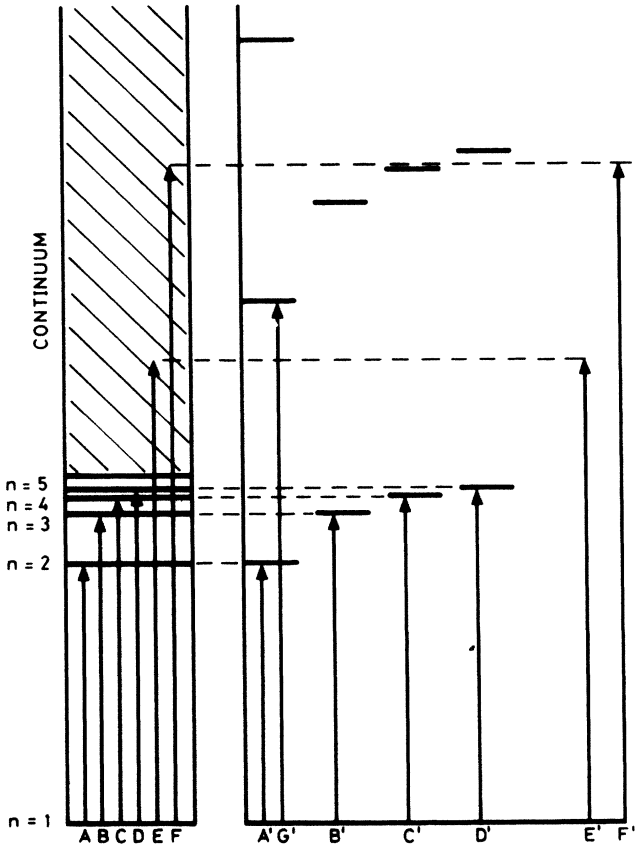

FIG. 13. Excitation spectrum for atomic hydrogen and a set of spectra from the harmonic-oscillator model. See text.

tation spectrum. However, there is no reason to expect the dipole oscillator strengths to provide the proper statistical weight.

XI. DISCUSSION

We have explored two aspects of the stopping properties of a spherical harmonic oscillator. First, the harmonic oscillator may serve as a reference standard for testing model theories of atomic stopping. The benefits are particularly simple scaling properties, an accurate tabulation of stopping cross section and straggling, and shell-correction expansions given to arbitrary order. Second, the results may be useful in predicing stopping cross sections and straggling parameters of atoms and molecules by means of an extension of Bohr's oscillator model of atomic stopping.

A. Model theories of atomic stopping

It is evident from Figs. 6–8 that the kinetic theory,[25] despite a difference in the shell-correction expansion from the second correction term on, yields accurate values for the stopping cross section down to velocities slightly below the stopping maximum, but increasing discrepancies at lower speed, in particular near and below the effective threshold, $2mv^2 \lesssim \hbar\omega/4$ for $m_1 \gg m$. This strengthens the validity of existing numerical evaluations of the kinetic scheme[23,24,51,52] as far as the medium and upper velocity range is concerned, but weakens the quantitative content of predictions made for the low-velocity range.[53] The qualitative content of the latter prediction is unaffected.[52]

Most useful is the observation that the kinetic theory rigorously predicts the first shell correction in the straggling parameter. Previous comparisons[25] involving the Fermi gas[40] as a reference standard did not reveal a straight equivalence. In fact, it was concluded[41] that of all moments over the energy-loss spectrum, the second was the only one where the validity of the kinetic scheme was questionable. This reservation can now be relaxed, except for the low-velocity region where the kinetic theory predicts M to be velocity proportional[25] while the Born approximation reveals a threshold (Fig. 14) similar to the one found for the stopping cross section (Fig. 8).

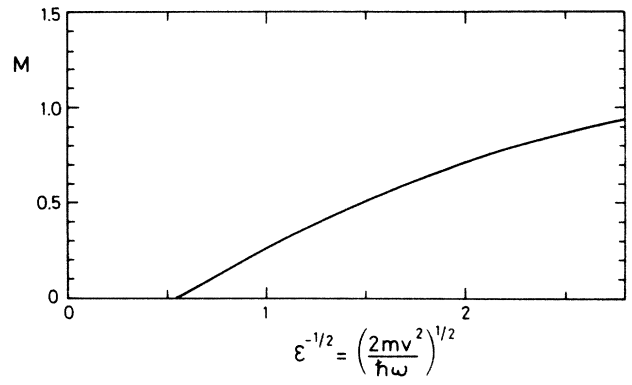

FIG. 14. Same as Fig. 5 with different abscissa scale.

The homogeneous Fermi gas has been included in the comparison *only* because it is a frequently used standard of reference. There is no reason to expect a close agreement with results for a harmonic oscillator. However, at a suitably chosen density, cf. Eq. (44), a meaningful comparison is possible, and characteristic differences become apparent (Fig. 10).

Inspection of Figs. 10 and 11 indicates, not surprisingly, that the harmonic oscillator is a more suitable system to model the stopping behavior of an atom than the Fermi gas, in particular in the velocity range around the stopping maximum.

The stopping properties of the Fermi gas have been utilized extensively in the local-density theory of stopping. The approach was initiated in Ref. 12 at a time when quantitative information on stopping power at moderate or low speed was essentially nonexistent, not to mention straggling. The model was utilized in the original spirit, in conjunction with statistical electron distributions, in Ref. 21, and the conclusion was that shell corrections can be evaluated reliably while evaluated mean ionization energies are more questionable. Major computational efforts, following the line of Ref. 22, were invested subsequently, without adequate improvement of the theoretical basis. Recently, the underlying oscillator strength spectra have been analyzed,[54] and the conclusion was that due to cancellation of errors, the stopping cross section can be evaluated in a feasible way from the dielectric scheme while higher moments would show increasingly pronounced discrepancies.

Evidently, the dielectric scheme has not been designed to describe the stopping properties of a one-electron system, nor is it particularly suitable for a system showing as pronounced a density gradient as a harmonic-oscillator electron distribution. Therefore, it appears justified to pay little attention to numerical discrepancies, such as a factor of 2 in the first shell correction of the straggling parameter, and consider those as "worst possible cases." More serious, however, are deviations from the rigorous scaling behavior, i.e., the occurrence of the factor $[\hbar\omega/(e^2/a_0)]^{1/4}$ in pertinent quantities. It indicates discrepancies for electron shells with $\hbar\omega \gg e^2/a_0$. The power $\frac{1}{4}$ prevents the discrepancies from becoming excessive, but we do find the occurrence of this parameter to be a rather disturbing feature.

Our calculations do not lend support to the binary-encounter model of atomic stopping at any velocity (Fig. 9).

B. Oscillator model of atomic stopping

The harmonic-oscillator model of atomic stopping was outlined by Bohr, well before the advent of quantum mechanics,[27,33,34] and was confirmed and quantified by Bethe.[1] The present form, Eq. (71), is an attempt to evaluate stopping cross sections on the basis of *dipole* oscillator strengths and transition energies only, down to velocities well below the limit of the Bethe asymptote Eq. (69). Thus, the input information does not go beyond what is needed to evaluate mean excitation energies.[55] Moreover, we also propose the same oscillator model to

apply to straggling, cf. Eq. (71').

In order to justify this approach, we have evaluated those terms in the shell-correction expansion for which generally valid expressions exist in the literature. In the case of the stopping cross section, the first shell correction turns out to be reproduced in full generality. The second shell correction comes out to be formally different from Fano's result,[2] but quantitatively in agreement in the case of hydrogen. In view of some reservations on the general validity of the close-encounter contribution to the second shell correction,[2] it is not evident whether Fano's or our expression has more general validity. Finally, the first shell correction to the straggling parameter agrees with Fano's, provided that account is taken of a term that obviously was omitted in Ref. 2.

It is not meaningful to carry out this comparison to higher shell corrections because of the occurrence of divergencies in the individual terms. Those show up in terms such as $\sum_n f_n(E_n-E_0)^3$ as singularities near the origin in configuration space and in terms such as $\langle v_2^6 \rangle$ at large target velocities. However, the agreement of the leading terms in the shell-correction expansion supplies some confidence to the approximate expressions for L and M, which evidently must be at least as accurate as the corresponding truncated shell-correction expansions. This has been tested on atomic hydrogen, where an adequate standard for comparison is available, with a satisfactory result, cf. Fig. 11.

C. Implications for stopping measurements

In view of Figs. 6–8, the present results are not expected to influence dramatically the predicted behavior of the stopping power down to about the maximum, as compared with predictions based upon the kinetic theory. With regard to lower velocities, some caution is indicated with regard to the magnitude of higher-order Born corrections as well as charge-changing collisions. Moreover, a lower limit of validity for the oscillator model, Eq. (69), has not been determined yet. On the other hand, for atoms heavier than hydrogen, the oscillator strength tends to be increasingly concentrated in mainly one excitation level plus the continuum.[56] Thus, near threshold where the continuum ceases to contribute, the oscillator model—with only the first excitation level being active—should give a reasonable description at least qualitatively. Figure 8 predicts an approximate straight-line behavior of the stopping power versus speed with an effective threshold near $2mv^2 \simeq \hbar\omega/4$, $\hbar\omega$ being the lowest excitation level.

This finding differs from the predictions of the dielectric theory,[57] as well as those of the kinetic theory.[25,53] For proton bombardment, and a minimum excitation level of a few eV, the effective threshold lies at a few 100-eV proton energy, i.e., in an energy range where moving protons are predominantly neutral and where stopping measurements are difficult to carry out, even in gases.

An experimental finding which may be related to our result has been reported for low-speed heavy ions penetrating gold foils and crystals.[58] A straight-line behavior consistent with Fig. 8 was observed with an extrapolated threshold in the range $(2-4)\times 10^8$ cm/s, dependent on the bombarding ion. This would be equivalent with an excitation level of $\hbar\omega \simeq 100-300$ eV, corresponding to the N and O shells which contain 32 and 18 electrons, respectively, i.e., all those electrons that may contribute to stopping in that velocity range except the conduction electrons which account for the velocity-proportional contribution to the stopping power.

XII. SUMMARY

(1) The Bethe stopping cross section for a penetrating fixed point charge has been evaluated for a spherical harmonic oscillator as a target; relativistic effects were disregarded. The stopping number approaches the well-known logarithmic dependence at high speed and shows an effective threshold at $2mv^2 \sim \hbar\omega/4$, ω being the resonance frequency. The stopping power has its maximum at $2mv^2 \simeq 4.5\hbar\omega$.

(2) The straggling parameter has been evaluated similarly. It approaches Bohr's value at high speed and shows a very weak Bethe-Livingston maximum at $2mv^2 \simeq 25\hbar\omega$.

(3) Shell-correction expansions have been derived to arbitrary order in powers of $\hbar\omega/2mv^2$ for both stopping cross section and straggling. Existing general expressions for first- and second-order shell corrections agree with our results, when specified to the harmonic oscillator.

(4) For light projectiles, i.e., positrons and electrons, the stopping cross section shows an oscillatory structure with discontinuities at integral values of $mv^2/2\hbar\omega$. The amplitude of the oscillations decreases as v^{-2}. Therefore, a shell-correction expansion has little meaning beyond the first term in the case of light projectiles.

(5) The shell-correction expansion is utilized to derive an equipartition rule for the stopping cross section in the case of heavy projectiles. It turns out that low-lying excitations contribute exactly one-half of the Bethe logarithm and of all nonvanishing orders of the shell-correction expansion, the other half being due to close encounters. Constant terms occur in both contributions which have opposite sign and equal magnitude and therefore cancel.

(6) The results can be compared with the predictions for a homogeneous Fermi gas, with the density chosen to match resonance frequency and mean-square velocity. Not unexpectedly, systematic differences show up at low and moderate projectile speeds.

(7) The kinetic theory of stopping, when applied to the oscillator, reproduces correctly the leading term in the shell corrections of both the stopping cross section and the straggling parameter. Total shell corrections agree very well with exact results for $2mv^2 \gtrsim \hbar\omega$, while a drastic difference is observed at lower speed. The kinetic theory predicts a velocity-proportional stopping power at low speed while the first Born approximation leads to an effective threshold at $2mv^2 \simeq \hbar\omega/4$.

(8) The local-density approximation has been applied to the density profile of a harmonic oscillator. Discrepancies must be expected when a statistical theory is applied to a one-electron system. It turns out that in addition to the occurrence of numerical differences, the scaling properties of both the stopping cross section and the straggling pa-

rameter are not reproduced.

(9) Following Bohr's oscillator model of atomic stopping, we tentatively express the stopping cross section of an atom or molecule as a weighted sum of harmonic-oscillator stopping cross sections with resonant frequencies corresponding to atomic transitions and dipole oscillator strengths as weight factors. This is in accordance with the Bethe asymptote, and it is demonstrated that this ansatz correctly describes the leading shell correction. The second shell correction is in agreement with the existing result (the generality of which is somewhat uncertain) in the case of atomic hydrogen.

(10) With this ansatz, the stopping number of atomic hydrogen has been evaluated and compared to the Born-approximation result. The agreement is very good down to about $2mv^2 \sim 4I$; substantial discrepancies are found at lower speed.

(11) The oscillator model has also been utilized as an ansatz for straggling. Also in this case, it turns out that the leading (logarithmic) shell correction is described correctly. A nonlogarithmic term, which has been omitted in the standard reference,[2] is shown to occur and is consistent with a previous result.[48]

(12) With some caution, the oscillator model is applied to low-velocity stopping, i.e., a velocity range where it has not been tested until now and where charge-changing collisions become crucial. A tentative explanation is given for an observed effective threshold for electronic stopping of heavy ions in gold, as reported by Moak *et al.*[58]

ACKNOWLEDGMENTS

Thanks are due to Pia Haagerup for help with the numerical computations and to J. R. Sabin, J. Oddershede, D. Semrad, and K. Johannessen for providing the results of unpublished numerical integrations. Professor P. Toennies kindly made us aware of Ref. 32. This work received partial support from the NATO Research Grants Program and from the Ingeborg and Leo Dannin Foundation, given to one of us (P.S.).

APPENDIX: OSCILLATIONS OF THE STOPPING NUMBER OF LIGHT PROJECTILES

According to Eqs. (9) and (10), the stopping number is $L(\epsilon)=\sum_{\nu=1}^{\infty} L_\nu(\epsilon)$, where

$$L_\nu(\epsilon)=\frac{1}{2(\nu-1)!}\int_{(\nu+\alpha t)^2 \leqq t/\epsilon} dt\, t^{\nu-2}e^{-t} \tag{A1}$$

and $\alpha=m/m_1$. If $4\alpha\nu\epsilon>1$, then $(\nu+\alpha t)^2>t/\epsilon$ for all t, and if $4\alpha\nu\epsilon<1$, the equation has two roots:

$$t_\nu^{\pm}=\frac{1-2\nu\alpha\epsilon\pm\sqrt{1-4\nu\alpha\epsilon}}{2\alpha^2\epsilon}\ . \tag{A2}$$

Note that the geometric mean is

$$(t_\nu^+ t_\nu^-)^{1/2}=\frac{\nu}{\alpha}\ . \tag{A3}$$

Therefore,

$$t_\nu^- < \frac{\nu}{\alpha} < t_\nu^+\ . \tag{A4}$$

The stopping number can now be written:

$$L(\epsilon)=\frac{1}{2}\sum_{\nu=1}^{1/4\alpha\epsilon}\frac{1}{(\nu-1)!}\int_{t_\nu^-}^{t_\nu^+} dt\, t^{\nu-2}e^{-t}\ . \tag{A5}$$

Let ν be a fixed positive integer. When

$$\frac{1}{\epsilon}=4\alpha\nu+h,\quad 0<h\ll 1 \tag{A6}$$

the νth term in L reads approximately

$$\begin{aligned} L_\nu(\epsilon) &\approx \frac{1}{2(\nu-1)!}(t_\nu^+ - t_\nu^-)(t^{\nu-2}e^{-t})_{t=\nu/\alpha} \\ &= \left[\frac{\alpha h}{2\pi}\right]^{1/2}\frac{\alpha^{-\nu}}{\nu}e^{(1-1/\alpha)\nu},\quad \nu\gg 1 \end{aligned} \tag{A7}$$

by Stirling's formula, while $L_\nu(\epsilon)=0$ for $1/\epsilon<4\alpha\nu$. Since all the other terms of $L(\epsilon)$ are smooth around $1/\epsilon=4\alpha\nu$, the factor $h^{1/2}$ indicates that $L(\epsilon)$ has square-root singularities at $1/\epsilon=4\alpha\nu$, $\nu=1,2,3,\ldots$. According to (A7), these singularities give rise to oscillations in $L(\epsilon)$ with an amplitude roughly proportional to

$$\left[\frac{\alpha^{-\nu}}{\nu}e^{(1-1/\alpha)\nu}\right]_{\nu=1/4\alpha\epsilon}, \tag{A8}$$

i.e., proportional to $\epsilon\exp[(1-1/\alpha-\ln\alpha)/4\alpha\epsilon]$. But for $\alpha\neq 1$, $1-1/\alpha-\ln\alpha<0$, so the amplitude of the oscillations decreases more rapidly than any power of ϵ for $\epsilon\to 0$.

However, for $\alpha=1$ the amplitude of the oscillations is proportional to ϵ. We shall not go through the details but quote the final formula,

$$L(\epsilon)=\ln\left[\frac{1}{2\epsilon}\right]-\epsilon g_1(\epsilon^{-1})+O(\epsilon^2)\ , \tag{A9}$$

where

$$g_1(\epsilon^{-1})=\frac{7+h}{2}+\frac{2}{\sqrt{\pi}}\sum_{l=0}^{\infty}\int_{h/2+l}^{\infty} dt\, t^{-1/2}e^{-t} \tag{A10}$$

and

$$\frac{1}{\epsilon}=4\nu+h \tag{A11}$$

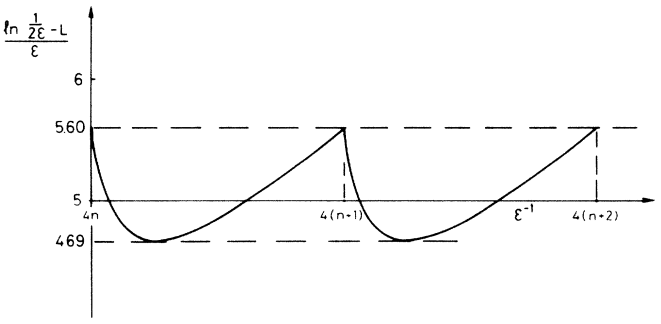

FIG. 15. Stopping of light projectiles (positrons and electrons). Asymptotic behavior of oscillatory structure in shell correction for $n \gg 1000$, with n being the number of excitable levels at a given energy.

with ν integer and $0 \le h \le 4$. The function $g_1(\epsilon^{-1})$ is shown in Fig. 15. It oscillates between 4.69 and 5.60 around the mean value 5.

The formula (A9) suggests that $L(\epsilon)$ has an asymptotic expansion of the form

$$L(\epsilon) = \ln\left[\frac{1}{2\epsilon}\right] - \sum_{n=1}^{\infty} \epsilon^n g_n(1/\epsilon) , \tag{A12}$$

where each g_i is a periodic function of period 4. It can be shown that only the mean values

$$\bar{g}_n = \tfrac{1}{4} \int_0^4 dt\, g_n(t) \tag{A13}$$

contribute to the residues of the Mellin transform $\bar{L}(s)$. Therefore,

$$\bar{g}_n = \frac{1}{n} \sum_{j=0}^{n} \begin{bmatrix} 2n \\ j \end{bmatrix} \mathfrak{S}_{2n+1-j}^{(n+1-j)} . \tag{A14}$$

In particular, $\bar{g}_1 = 5$ and $\bar{g}_2 = 29.5$. The functions g_n are hard to compute explicitly for $n \ge 2$. By some rough numerical computations, we found that g_2 oscillates between 29 and 30. Therefore, it is probably quite safe to put $g_n \approx \bar{g}_n$ for $n \ge 2$.

[1] H. Bethe, Ann. Phys. (Leipzig) **5**, 325 (1930).
[2] U. Fano, Annu. Rev. Nucl. Sci. **13**, 1 (1963).
[3] M. Inokuti, Rev. Mod. Phys. **43**, 297 (1971).
[4] H. A. Bethe and R. W. Jackiw, *Intermediate Quantum Mechanics* (Benjamin, New York, 1968).
[5] P. Sigmund, in *Radiation Damage Processes in Materials,* edited by C. H. S. Dupuy (Noordhoff, Leiden, 1975), p. 3.
[6] M. S. Livingston and H. A. Bethe, Rev. Mod. Phys. **9**, 264 (1937).
[7] H. A. Bethe, L. M. Brown, and M. C. Walske, Phys. Rev. **79**, 413 (1950).
[8] L. M. Brown, Phys. Rev. **79**, 297 (1950).
[9] M. C. Walske and H. A. Bethe, Phys. Rev. **83**, 457 (1951).
[10] M. C. Walske, Phys. Rev. **88**, 1283 (1952).
[11] J. Lindhard and M. Scharff, Phys. Rev. **85**, 1058 (1952).
[12] J. Lindhard and M. Scharff, K. Dan. Vidensk. Selsk. Mat. Fys. Medd. **27**, No. 15 (1953).
[13] U. Fano and J. E. Turner, *Studies in Penetration of Charged Particles in Matter,* National Academy of Sciences—National Research Council, Washington, D.C., Publication No. 1133, 1964, p. 49. (Available from National Academy of Sciences, Printing and Publicity Office, 2101 Constitution Ave., Washington, D.C. 20418.)
[14] H. H. Andersen, H. Sørensen, and P. Vajda, Phys. Rev. **180**, 373 (1969).
[15] M. C. Walske, Phys. Rev. **88**, 1283 (1952).
[16] G. S. Khandelwal, Phys. Rev. A **26**, 2983 (1982).
[17] H. Bichsel, Phys. Rev. A **28**, 1147 (1983).
[18] E. J. McGuire, Phys. Rev. A **26**, 1858 (1982); **28**, 49 (1983).
[19] J. Lindhard, K. Dan. Vidensk. Selsk. Mat. Fys. Medd. **28**, No. 8 (1954).
[20] J. Lindhard and A. Winther, K. Dan. Vidensk. Selsk. Mat. Fys. Medd. **34**, No. 4 (1964).
[21] E. Bonderup, K. Dan. Vidensk. Selsk. Mat. Fys. Medd. **35**, No. 17 (1967).
[22] W. K. Chu and D. Powers, Phys. Lett. **40A**, 23 (1972).
[23] J. R. Sabin and J. Oddershede, Phys. Rev. A **26**, 3209 (1982).
[24] J. R. Sabin and J. Oddershede, Phys. Rev. A **29**, 1757 (1984).
[25] P. Sigmund, Phys. Rev. A **26**, 2497 (1982).
[26] H. Bichsel, M. Inokuti, and D. Y. Smith, Phys. Rev. A **33**, 3567 (1986).
[27] N. Bohr, Philos. Mag. **25**, 10 (1913).
[28] J. C. Ashley, R. H. Ritchie, and W. Brandt, Phys. Rev. A **8**, 2402 (1973).
[29] J. Lindhard, Nucl. Instrum. Methods **132**, 1 (1976).
[30] K. W. Hill and E. Merzbacher, Phys. Rev. A **9**, 156 (1974).
[31] H. Esbensen, thesis, Universitet Aarhus, 1976.
[32] M. S. Bartlett and J. E. Moyal, Proc. Cambridge Philos. Soc. **45**, 545 (1949).
[33] N. Bohr, Philos. Mag. **30**, 581 (1915).
[34] N. Bohr, Z. Phys. **34**, 142 (1925).
[35] L. I. Schiff, *Quantum Mechanics* (McGraw-Hill, New York, 1981).
[36] *Tables of Integral Transforms I* (Bateman Manuscript Project), edited by A. Erdelyi (McGraw-Hill, New York, 1954).
[37] *Handbook of Mathematical Functions,* edited by M. Abramowitz and I. A. Stegun (Dover, New York, 1965).
[38] E. Bonderup and P. Hvelplund, Phys. Rev. A **4**, 562 (1971).
[39] J. Oddershede and J. R. Sabin (private communication).
[40] P. Sigmund and D. J. Fu, Phys. Rev. A **25**, 1450 (1982).
[41] P. Sigmund and K. Johannessen, Nucl. Instrum. Methods B **6**, 486 (1985).
[42] E. Gerjuoy, Phys. Rev. **148**, 54 (1966).
[43] J. J. Thomson, Philos. Mag. **23**, 449 (1912).
[44] E. Kührt and R. Wedell, Phys. Lett. **86A**, 54 (1981); **97A**, 347 (1983); Phys. Status Solidi B **116**, 585 (1983).
[45] D. Semrad (private communication).
[46] W. K. Chu, Phys. Rev. A **13**, 2057 (1976).
[47] F. Besenbacher, J. U. Andersen, and P. Hvelplund, Nucl. Instrum. Methods **168**, 1 (1980).
[48] P. Hvelplund (unpublished).
[49] K. Johannessen (private communication).
[50] J. E. Turner, quoted in Ref. 2.
[51] J. Oddershede and J. R. Sabin, At. Data Nucl. Data Tables **31**, 275 (1984).
[52] J. R. Sabin, J. Oddershede, and P. Sigmund, Nucl. Instrum. Methods B **12**, 80 (1985).
[53] J. Oddershede, J. R. Sabin, and P. Sigmund, Phys. Rev. Lett. **51**, 1332 (1983).
[54] R. E. Johnson and M. Inokuti, Comments At. Mol. Phys. **14**, 19 (1983).
[55] J. L. Dehmer, M. Inokuti, and R. P. Saxon, Phys. Rev. A **12**, 102 (1975).
[56] U. Fano and J. W. Cooper, Rev. Mod. Phys. **40**, 441 (1968).
[57] J. Lindhard and M. Scharff, Phys. Rev. **124**, 128 (1961).
[58] C. D. Moak, B. R. Appleton, J. A. Biggerstaff, M. D. Brown S. Datz, T. S. Noggle, and H. Verbeek, Nucl. Instrum. Methods **132**, 95 (1976).